

N O T I C E

THIS DOCUMENT HAS BEEN REPRODUCED FROM
MICROFICHE. ALTHOUGH IT IS RECOGNIZED THAT
CERTAIN PORTIONS ARE ILLEGIBLE, IT IS BEING RELEASED
IN THE INTEREST OF MAKING AVAILABLE AS MUCH
INFORMATION AS POSSIBLE

NASA TECHNICAL MEMORANDUM

NASA TM-82412

LOW DRAG ATTITUDE CONTROL FOR SKYLAB ORBITAL LIFETIME EXTENSION

By John R. Glaese and Hans F. Kennel
Systems Dynamics Laboratory

April 1981



NASA

*George C. Marshall Space Flight Center
Marshall Space Flight Center, Alabama*

(NASA-TM-82412) LOW DRAG ATTITUDE CONTROL
FOR SKYLAB ORBITAL LIFETIME EXTENSION (NASA)
65 p HC A04/MF A01 CSCL 22A

N81-22074

Unclass
G3/15 42152

1. REPORT NO. NASA TM-82412		2. GOVERNMENT ACCESSION NO.		3. RECIPIENT'S CATALOG NO.	
4. TITLE AND SUBTITLE Low Drag Attitude Control For Skylab Orbital Lifetime Extension				5. REPORT DATE April 1981	
				6. PERFORMING ORGANIZATION CODE	
7. AUTHOR(S) John R. Glaese and Hans F. Kennel				8. PERFORMING ORGANIZATION REPORT NO.	
9. PERFORMING ORGANIZATION NAME AND ADDRESS George C. Marshall Space Flight Center Marshall Space Flight Center, Alabama 35812				10. WORK UNIT NO.	
				11. CONTRACT OR GRANT NO.	
12. SPONSORING AGENCY NAME AND ADDRESS National Aeronautics and Space Administration Washington, D.C. 20546				13. TYPE OF REPORT & PERIOD COVERED Technical Memorandum	
				14. SPONSORING AGENCY CODE	
15. SUPPLEMENTARY NOTES Prepared by Systems Dynamics Laboratory, Science and Engineering					
16. ABSTRACT In the fall of 1977 it was determined that Skylab had started to tumble and the original orbit lifetime predictions were much too optimistic. A decision had to be made whether to accept an early uncontrolled reentry with its inherent risks or try to attempt to control Skylab to a lower drag attitude in the hope that there was enough time to develop a Teleoperator Retrieval System, bring it up on the Space Shuttle and then decide whether to boost Skylab to a higher longer life orbit or to reenter it in a controlled fashion. In the following the end-on-velocity (EOVV) control method is documented, which was successfully applied for about half a year to keep Skylab in a low-drag attitude with the aid of the control moment gyros and a minimal expenditure of attitude control gas.					
17. KEY WORDS Angular Momentum Management Attitude Control Control Moment Gyros (CMG's) Quaternions Spacecraft Skylab Steering Law				18. DISTRIBUTION STATEMENT Unclassified-Unlimited	
19. SECURITY CLASSIF. (of this report) Unclassified		20. SECURITY CLASSIF. (of this page) Unclassified		21. NO. OF PAGES 64	
				22. PRICE NTIS	

ACKNOWLEDGEMENTS

We hereby express our appreciation for the excellent support we received in the simulation area from the MSFC simulation division, especially Mr. Jack Lucas and Dr. Frank Hay of MSFC and Mr. Ray Nix of Honeywell.

TABLE OF CONTENTS

	Page
INTRODUCTION	1
ATTITUDE AND POINTING CONTROL SYSTEM (APCS).....	2
CMG CONTROL SYSTEM	4
EOVV MOMENTUM CONTROL.....	4
IOP Momentum Control.....	6
POP Momentum Control.....	8
EOVV STRAPDOWN UPDATE	10
EOVV OPERATION AND PERFORMANCE.....	12
APPENDIX A.....	16
APPENDIX B.....	19
APPENDIX C.....	22
APPENDIX D.....	31
APPENDIX E.....	37
APPENDIX F.....	53
APPENDIX G.....	55
APPENDIX H.....	56
REFERENCES	60

~~REPEATING PAGE BLANK NOT FILMED~~

LIST OF ILLUSTRATIONS

Figure	Title	Page
1.	Skylab.....	2
2.	CMG mounting arrangement	5
3.	POP command superposition	9
4.	Orbital Y-momentum control.....	11
5.	Sun elevation angle beta (April 1978/August 1979)	13
6.	Orbital Y-momentum	14
A-1.	Coordinate systems	17
C-1.	Motion of I Coordinate System	29

TECHNICAL MEMORANDUM

LOW DRAG ATTITUDE CONTROL FOR SKYLAB ORBITAL LIFETIME EXTENSION

INTRODUCTION

On February 9, 1974, Skylab systems were configured for a final power down and Skylab was deactivated in a passively stabilized gravity gradient (GG) attitude with the Multiple Docking Adapter (MDA) up and the solar panels trailing (Fig.1). Prediction of solar cycle 21 activity (the solar cycle predicted to begin in 1977) indicated that this attitude would result in a potential storage period of 8 to 10 yr. However, in the fall of 1977 it was determined that Skylab had started to tumble randomly and was experiencing an increased orbital decay rate. This was the result of the greater than predicted solar activity at the beginning of solar cycle 21. This increased activity increased the drag forces on the vehicle. Skylab was now predicted to reenter the Earth's atmosphere in late 1978 or early 1979 unless something was done to reduce the drag forces acting on it. It was necessary to make a decision to either accept an early uncontrolled reentry (and with it the danger that relatively large pieces could damage something or hurt somebody) or to attempt to actively control Skylab in a lower drag attitude thereby extending its orbital lifetime until a Space Shuttle mission could effect a boost or deorbit maneuver with Skylab.

In order to verify what options could be accomplished with the on-board Skylab systems, in March 1978 a team of NASA engineers went to the Bermuda ground station to establish communications. The resulting data indicated no discernible degradation of the Skylab systems during its four years of orbital storage. The knowledge that Skylab was in an unstable tumble prompted investigation into schemes which might extend the orbital lifetime of Skylab.

The first option investigated was to use the on-board thruster attitude control system (TACS) to maintain a quasistable tumble. However, it was soon determined that this option would not extend the lifetime sufficiently to correspond to the operational readiness of the Space Shuttle for a possible reboost or deorbit mission. The only alternative was to reactivate and continuously control the Skylab in a minimum drag attitude. In order to accomplish this, the low-drag, end-on-velocity-vector (EOVV) attitude control scheme was developed in record time (the authors were given the task on March 20 and the scheme was flown on July 11). Skylab remained in the low-drag attitude until January 25, 1979, when the vehicle was commanded to its original design attitude [solar inertial (SI)], which was a high-drag attitude (See Skylab EOVV Time table for further details).

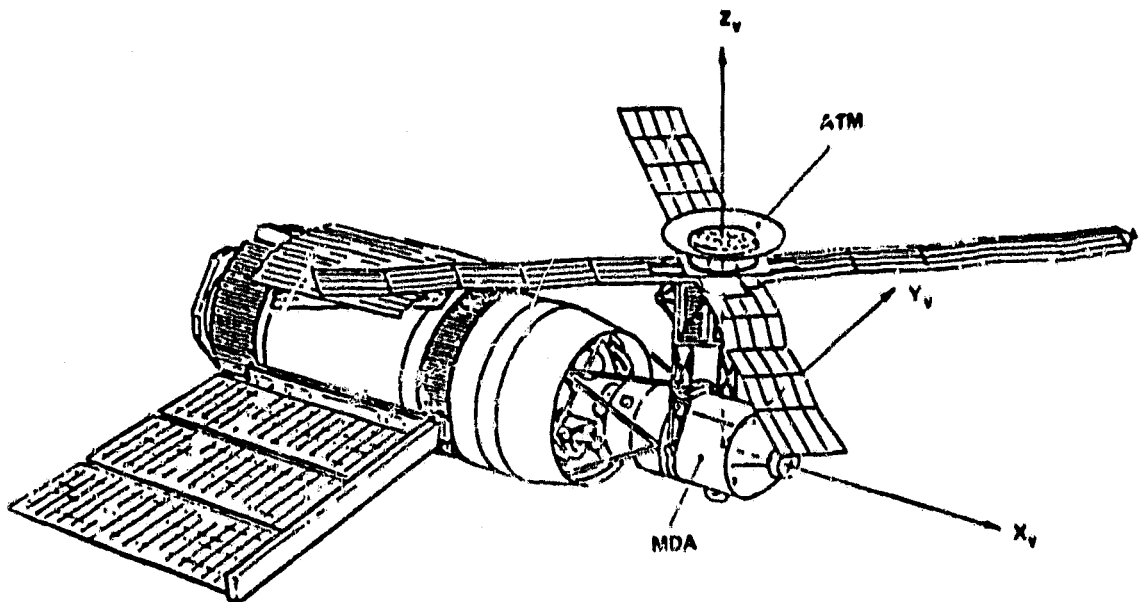


Figure 1. Skylab.

With the active control of Skylab in the low-drag attitude, it was decided to accelerate the development of an orbital retrieval system (Teleoperator Retrieval System) that might be accommodated on an early flight of the Space Shuttle, thus increasing the chances of rendezvousing with Skylab. The rate of orbital decay, however, continued to increase due to the increased solar activity. Skylab's on-board systems also showed signs of deterioration, and there were strong indications that the schedule of the Space Shuttle would slip. For these reasons, the effort for a Skylab recovery was terminated in December 1978, and Skylab was placed in the SI attitude in January 1979. In this attitude the ground maintenance was minimum and efforts could be concentrated on a method for a controlled reentry of Skylab [1].

More detail about the reactivation mission can be found in Reference 2. The following section gives the development of the EOVS control scheme.

ATTITUDE AND POINTING CONTROL SYSTEM (APCS)

The control of the Skylab attitude to the attitude reference was done exactly as in the original mission [3]. However, only the pointing control system (PCS) of the APCS was used; the experiment pointing control system (EPCS) was disabled.

The major parts of the APCS were the rate gyros, the Acquisition Sun Sensors (ACQ SS), the Star Tracker (it had failed during the

SKYLAB EOVV TIMETABLE

3/20/78 Authors made aware that a low-drag attitude momentum management method was needed.

4/ 7/78 Concept review by MSFC middle management.

4/26/78 Final equations for 2-CMG EOVV to IBM.

5/22/78 Documentation on ATMDG software change requirements for 2-CMG EOVV operation completed by IBM.

6/ 8/78 CMG spin up in caged position (7:00 am CST, caged to H+[1.92 0.03 0.36])

6/ 9/78 7 am CDT. Rotation about sunline to place x axis IOP.
8 am CDT. CMG control in SI attitude.
12 noon CDT. Loss of control due to inadvertent servo power cut-off to CMG#3 (faulty switch selector introduced additional command)
1 pm CDT. Retained control with CMG's after 2 orbits.

6/11/78 8:27 UT. Entering EOVV A attitude.

6/28/78 Loss of EOVV attitude control due to large angular momentum and CMG saturation.

7/ 5/78 Re-establishment of EOVV A attitude.

7/ 9/78 Loss of all power introduces loss of attitude control.

7/19/78 Reorientation maneuver to find attitude.

7/25/78 Re-establishment of EOVV A attitude.

11/ 4/78 Maneuver from EOVV A to EOVV F attitude

12/19/78 NASA HQ press conference (J.Yardley/W.Aller) where Skylab is declared unsavable.

1/25/79 Reorientation maneuver to SI attitude (hold mode to allow time for the design of the torque equilibrium control method for reentry).

original mission), the Apollo Telescope Mount Digital Computer (ATMDC), the Workshop Computer Interface Unit (WCIU), three double-gimbaled Control Moment Gyros (CMGs), and cold-gas (compressed nitrogen) Thruster Attitude Control System (TACS).

Six control modes were addressable: (1) STANDBY, (2) SOLAR INERTIAL (SI), (3) EXPERIMENT POINTING, (4) ATTITUDE HOLD/CMG, (5) ATTITUDE HOLD/TACS, (6) ZLV (for z axis along the local vertical). EOVV control was programmed to be a substate of the ZLV mode. The basic ZLV attitude was with the positive z axis along the local vertical, pointing up, and the positive x axis in the orbital plane, pointing in the direction of the velocity vector. Any angular offset from the basic ZLV attitude (offset identified by the quaternion Q_0) could be commanded by a set of three Euler angles (χ 's) with a y,z,x, rotation sequence. None of the original APCS capabilities were eliminated by the addition of the EOVV control method.

CMG CONTROL SYSTEM

The CMG control system was composed of three orthogonally mounted, double gimbaled CMGs with angular momentum magnitude H of 3050 Nms (2280 ft-lb-sec) as shown in Figure 2. The CMG control law utilized three normalized torque commands and the CMG momentum status to generate the proper CMG gimbal rate commands [4]. The CMG control law consisted of three parts: CMG steering law, rotation law, and gimbal stop avoidance logic. There also were some other routines for specialized situations like caging the CMGs to a desired momentum state [5].

The CMG control law had the capability to operate with either three or two CMG's for redundancy. Since CMG No.1 had failed during the original Skylab mission the CMG control law was always in the two-CMG option.

EOVV MOMENTUM CONTROL

The problem for EOVV was to determine variable reference attitudes such that, on the average, the angular momentum was contained within the two-CMG capability (allowing the CMGs to hold the prescribed attitude reference), while the average reference attitude was consistent with the desired low aerodynamic drag.

Minimizing the drag on Skylab required that the least frontal area was presented to the wind while at the same time holding a GG torque equilibrium (at the altitudes of concern the GG torques were still very dominant and they were therefore used exclusively for momentum control;

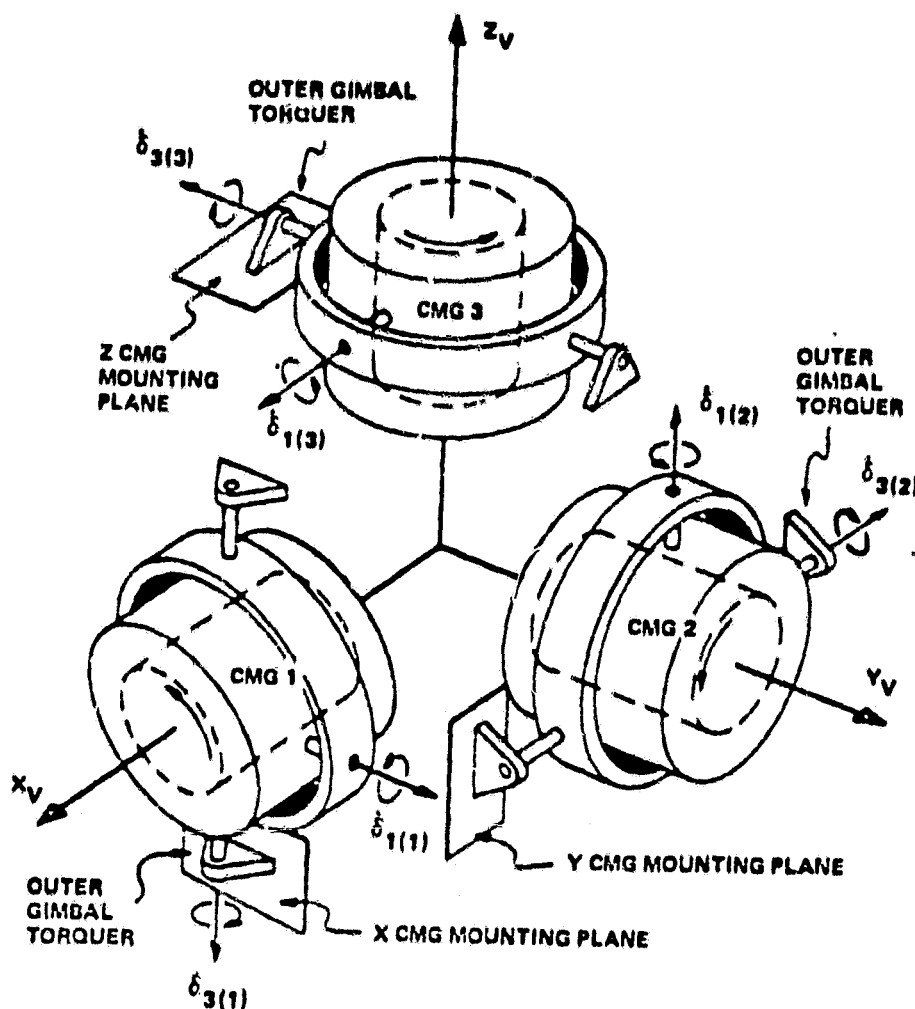


Figure 2. CMG mounting arrangement.

for details on the aerodynamic torques, [1]). Keeping the minimum principal moment of inertia axis parallel to the wind direction fulfilled this requirement. To have the necessary electrical power from the solar cells as well as strapdown update information from the ACQ SS, the Skylab was rolled through the angle η_{xn} (APPENDIX F) about the minimum principal moment-of-inertia axis (principal x axis) such that once per orbit the sun line passed nominally through the center of the ACQ SS.

There were two attitudes which satisfied these requirements: One with the MDA forward (EOVV A) and one with the MDA backward (EOVV B). In either case, the MDA had to be pitched down by a varying amount (depending on the solar elevation angle $\beta \approx -\eta_x$ above the orbital plane) to align the principal x axis with the orbit tangent.

Control of the angular momentum was split into the control of the momentum component perpendicular to the orbital plane (POP control) and the component in the orbital plane (IOP control). Since IOP control had some effect on POP control, IOP control is treated first.

IOP Momentum Control

When Skylab was originally designed, it was desirable to minimize the GG torques about the minimum principal-moment-of-inertia axis as much as possible since the momentum management scheme [6] was least efficient about this axis. For EOVS control this meant that there were basically no large GG torques available about this axis and, furthermore, there would be no change in torques when the principal y or z axes were ± 45 degrees from the orbital plane (tracking of the sun by rolling about the x axis would make this a frequent occurrence). Therefore this first order effect had to be abandoned. The actually used momentum control scheme assumed that the Skylab moments-of-inertia were cylindrical, with an average moment-of-inertia difference of ΔI .

The problem was solved by using a second order effect. First, a large cyclic POP torque was generated by "nodding" (pitching) the Skylab in the orbital plane. Cyclic nodding was required to avoid a continuous momentum build-up in the POP direction. The cyclic POP torque was then tilted as required (differently for each half cycle or quarter orbit) to generate a controllable component in the orbital plane. The second order effect stems from the fact that the IOP torque is proportional to the nodding angle times the tilting angle.

The effectiveness of the IOP momentum control did not depend on the frequency of the nodding. However, other considerations entered: (1) the lower the frequency, the larger the POP momentum swing, and (2) the higher the frequency, the larger the maneuver momentum that has to be exchanged between the vehicle and the CMG system. Since only a limited momentum volume was available with two CMGs and their associated gimbal stop problems, a nodding frequency of twice orbital frequency was chosen as a viable compromise ($s \equiv \sin$)

$$\eta_{yn} = - \eta_{ym} s(2\Omega_o t - \eta_o) \quad (1)$$

Therefore, the IOP momentum control calculations were done every quarter orbit. This had the added advantage that the resolution from the nearly inertial O system to the rotating L system happened in 90 degree intervals allowing indexing of some of the saved momentum samples rather than requiring a full-fledged resolution.

To minimize transients at the quarter orbit sample points, the tilting angle was also sinusoidal with twice orbital frequency and its amplitude was the only changing quantity:

$$\eta_{zn} = - \eta_{zm} s (2\Omega_o t - \eta_o) \quad , \quad (2)$$

where

$$\eta_{zm} = K_{\eta z} (e_{zo} - e_a + e_r/4)$$

$$K_{\eta z} = (15H)/(48\eta_{ym}\Omega_o\Delta I)$$

e_{zo} = momentum component to be desaturated

e_a = amplitude

e_r = ramp per orbit .

The phasing of the nodding and tilting angles was the same so that the amplitude was reached half-way between sample points.

The sample points were chosen so that one of the samples (sample 2) occurred at the time when the sun was perpendicular to the solar panels. This happened before orbital noon for EOVB A and after noon for EOVB B (the difference of about 11 degrees between the geometric and the principal x axes is the reason). In addition the nodding rate, being added to the orbital rate, was phased so that it slowed Skylab down when the solar panels were perpendicular to the sun and therefore maximized the power from the solar panels [giving rise to the minus signs in equation (1) and equation (2)].

The tilting angle amplitude was calculated so that the IOP momentum component, which could be affected during the next quarter orbit (it was along the direction of the connecting line between the present sample point and the next one), would be driven to the desired value. The desired value was basically zero, but any constant torque in the L system caused only a cyclic momentum change (with normalized amplitude e_a) over one orbit and should not be compensated for. Therefore, the momentum attributable to a constant L system torque was subtracted out of the momentum e_{zo} to be desaturated over the next quarter orbit.

To recognize a cyclic as well as a ramp momentum change, four past momentum samples were saved. The samples were also used to generate strapdown update information once an orbit (flow charts in APPENDIX H).

POP Momentum Control

The torques associated with a rotation about the orbit normal are much stronger than the ones associated with IOP control. Hence, the momentum sampling for POP control has to be done as frequently as possible. However, the transients should have had a chance to settle before the next POP sample is taken. Twelve samples per orbit satisfied both requirements. The desaturation gain (APPENDIX D.b)

$$K_{yc} = H / (3\omega_o^2 \Delta I T_{des}) \quad , \quad (3)$$

is calculated so that a step attitude change of

$$\eta_{yc} = K_{yc} \Delta e_y \quad , \quad (4)$$

desaturates the desired Δe_y in one desaturation interval. To further reduce transients, the calculated POP angle (which would have eliminated the momentum offset within the next desaturation interval if the angle were applied fully during the interval) was ramped in so that the angle was achieved at the end of the interval. Since this only reduced the momentum offset by half, the angle was ramped-out during the following interval for a full momentum offset elimination. The ramp due to the newly calculated POP angle was simply superimposed on the ramp-down from the previous POP angle (Fig. 3). The attitude command is, therefore, given by (N signifies the present and N-1 the past value)

$$\begin{aligned} (\eta_{yc})_N &= K_{yc} [(\Delta e_y)_N - 0.5 (\Delta e_y)_{N-1}] \\ &= K_{yc} (\Delta e_y)_N - 0.5 (\eta_{yc})_{N-1} \quad . \end{aligned} \quad (5)$$

The ramps connecting the η_{yc} 's are generated by

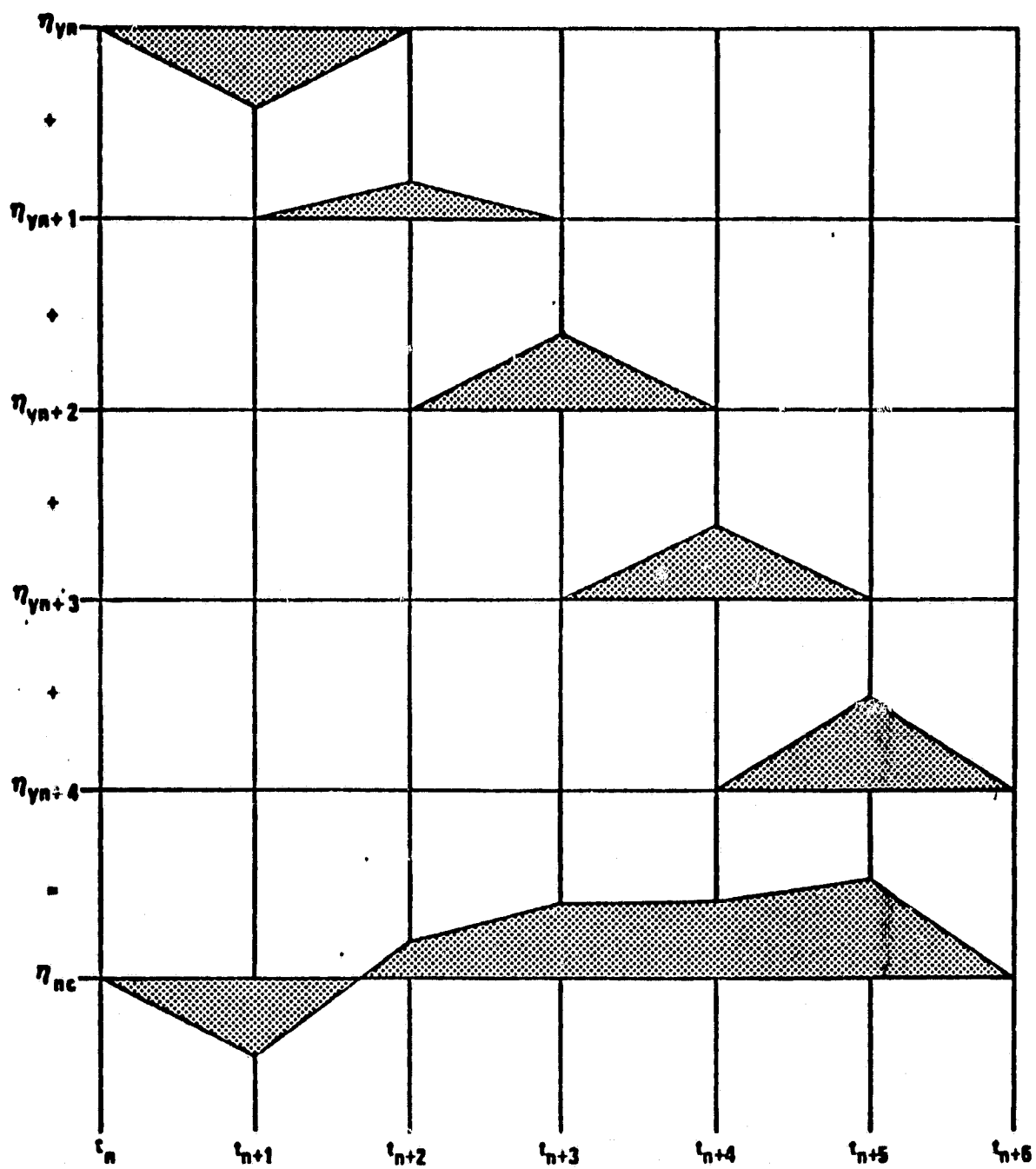


Figure 3. POP command superposition.

$$(\eta_y)_N = (\eta_y)_{N-1} + \Delta \eta_y \Delta t \quad , \quad (6)$$

where

$$\Delta \eta_y = [(\eta_{yc})_N - (\eta_{yc})_{N-1}] / T_{des} \quad .$$

This method resulted in a constant hang-off when necessary: The angle change due to the old angle being ramped-out was compensated by the ramp-in of the new angle (in flight, constant hang-offs were common due to strapdown and navigation errors and they were not detrimental, since the momentum control kept the vehicle at the truly desired attitude). A block diagram of the EOVV orbital y momentum control scheme is shown in Figure 4.

EOVV STRAPDOWN UPDATE

Strapdown updates about the vehicle x and y axes were always furnished by the ACQ SS. To do that, the roll angle about the principal x axis was changed by large amounts to compensate for the large beta angle changes (a slow change) and relatively fast smaller corrections were applied to compensate for the nodding and the tilting angles. The overall effect was that the vehicle z axis nominally traced a cone about orbital north. The difference between where the sun-line was at the closest approach to the ACQ SS center and where it was supposed to be according to the strapdown information gave the strapdown x and y information.

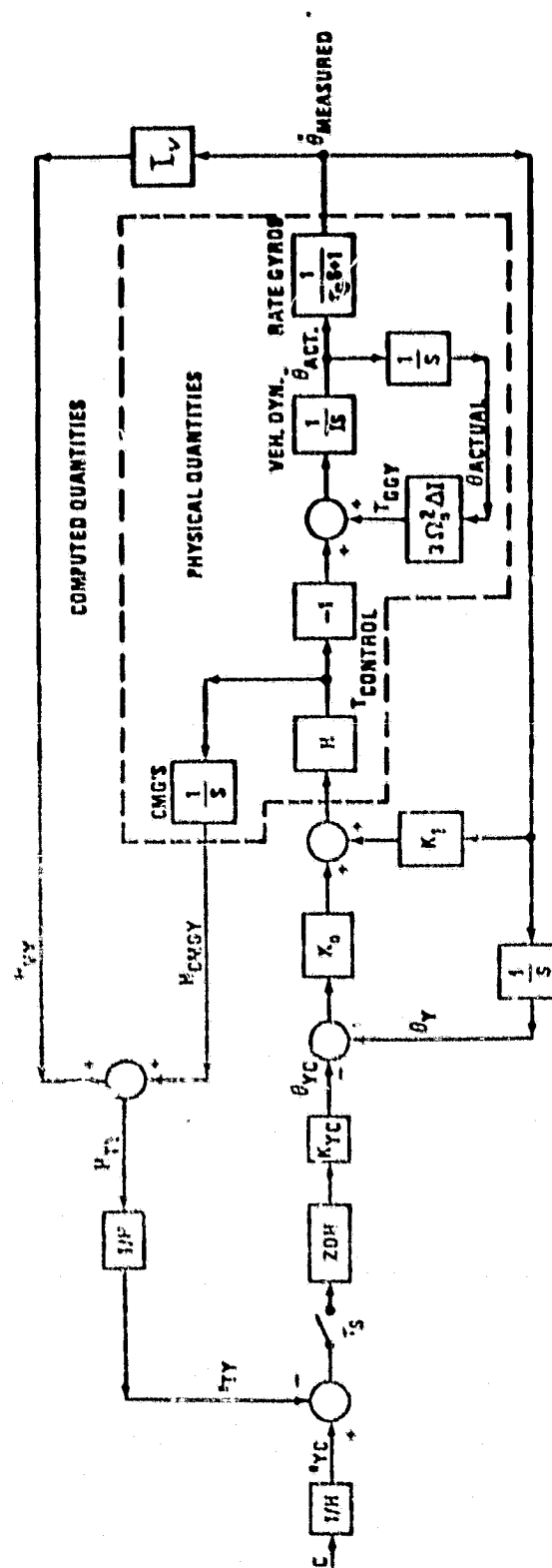
Since there was no other sensor available, it was more difficult to gain strapdown update information about the sun-line. The selected momentum control method, fortunately, had the feature that, due to the nodding angle, a misalignment between the ideal orbital plane and the indicated orbital plane generated an IOP momentum ramp.

The actual strapdown update was done by changing the reference quaterion (APPENDIX H.6)

$$Q_{VI} = \overline{\overline{\Delta Q}} Q_{VI} \quad , \quad (7)$$

where the double-bar operator is defined in APPENDIX E and

$$\Delta Q = [\Delta Q_1, \Delta Q_2, \Delta Q_3, \Delta Q_4] = [\underline{\Delta Q}, \Delta Q_4] \quad , \quad (8)$$



$\tau_S \approx 450S: K_{YC} = \frac{H}{3\Omega^2 \Delta I \tau_S}: \Delta I = \frac{1}{2}(I_{PY} + I_{PL}) - I_{PY}: K_{YC} \text{ \& } K_i \text{ ARE NOMINAL CONTROL GAINS}$
 $H = 3050 \text{ NMS (NOMINAL CMG MOMENTUM)}: \tau_G \text{ REPRESENTS RATE GYRO LAG}: \Omega_g \text{ IS ORBITAL RATE}$

Figure 4. Orbital Y-momentum control.

with

$$\underline{\Delta Q} = 0.5 (\underline{s} \times \underline{v} + \mu_z \underline{s}) \quad , \quad (9)$$

and

$$\Delta Q_4 = \sqrt{1 - \underline{\Delta Q} \cdot \underline{\Delta Q}} \quad . \quad (10)$$

The cross product in equation (9) is the ACQ SS update and the last term is the IOP ramp update, where \underline{v} is a unit vector in the sun direction as calculated by the ATMDC and \underline{s} is the measured sun direction unit vector. μ_z is the angle about the measured sun direction (the gain $K_{\mu z}$ is developed in APPENDIX D.e.);

$$\mu_z = - K_{\mu z} (e_{TLN1} - e_{TLN1P}) \quad , \quad (11)$$

where $K_{\mu z}$ is a gain and $(e_{TLN1} - e_{TLN1P})$ is the angular momentum change (ramp) per orbit (μ_z is calculated at sample point 1) modified by the ground commanded ramp bias e_{rb} since

$$e_{TLN1P} = e_{TLN1P} + e_{rb} \quad , \quad (12)$$

is calculated right after the μ_z calculation and, therefore, is used for the next μ_z calculation (e_{TLN1P} is modified at every sample point to account for the momentum changes commanded by η_{zm}).

EOVV OPERATION AND PERFORMANCE

The original EOVV equation considered EOVV A only. In EOVV A CMG No. 2 received more solar radiation when the sun was north of the orbital plane (positive beta angle) and less when it was south of the orbital plane (negative beta angle). For large negative beta angles the CMG No. 2 bearing temperatures became critically low. As a consequence, the EOVV A equations had to be modified during EOVV operation to allow an EOVV B attitude during extended periods of large negative beta angles (Fig. 5).

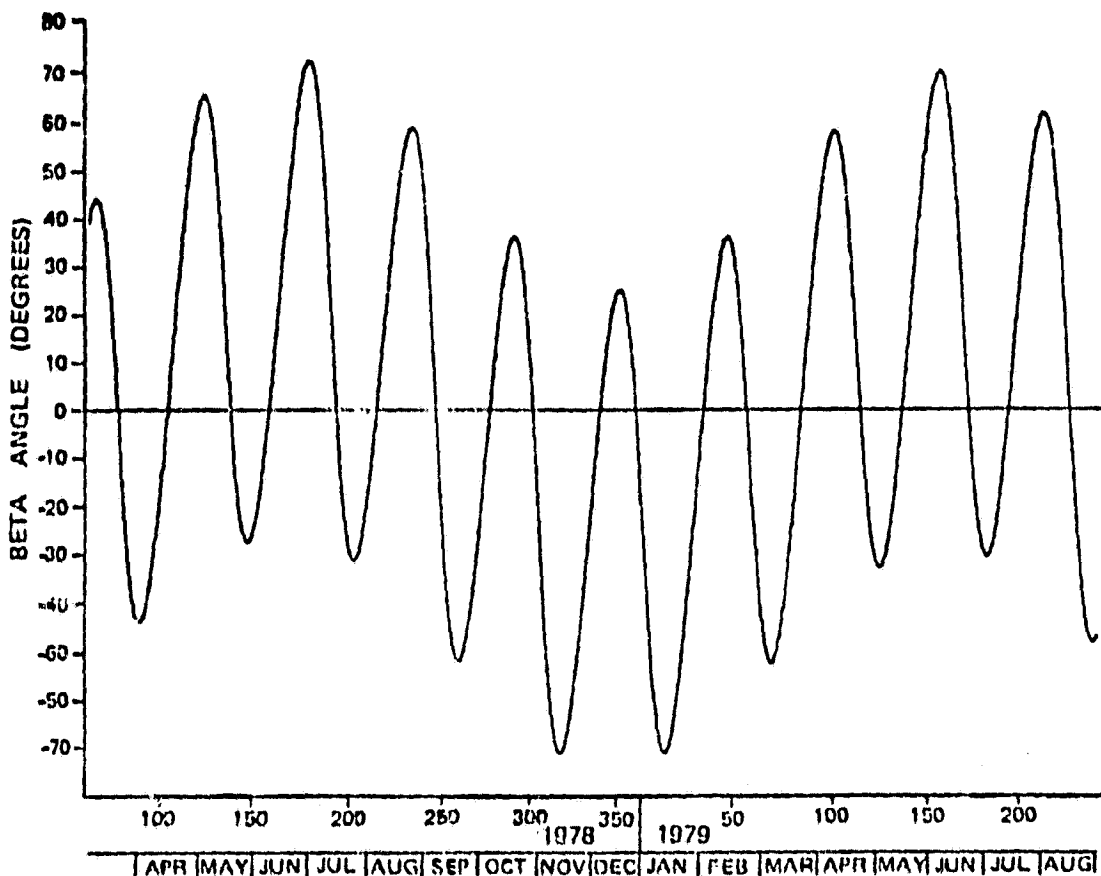


Figure 5. Sun elevation angle beta (April 1978/August 1979).

Constant η_{yc} angle hang-offs (caused by strapdown, navigation, and other errors) required constant POP momentum hang-offs to generate the necessary commands. Since the range of acceptable POP momentum component was rather limited ($\pm 0.4H$ from the nominal; the nominal e_{TN} being $2.5H$ in EOVB A and $0.3H$ in EOVB B) the nominal POP momentum had to be changed to accept large angle hang-offs (3 deg of POP angle hang-off required $0.1H$ POP momentum hang-off). This change in nominal momentum was made from the ground at the beginning of the EOVB operation and later was automated on-board to guard against ground inattention, ground system failures, and long telemetry coverage gaps (Fig. 6.). Momentum excursions outside the specified range caused loss of attitude due to CMG saturation on one occasion June 28, 1978, and it was therefore very important to keep the POP momentum bounded.

Strapdown updating about the sun-line was done with information derived from the IOP momentum ramp. Unfortunately, the evaluation of the IOP momentum ramp yielded very noisy readings from one orbit to the next and could only be used with a very reduced gain $K_{\mu z}$. This,

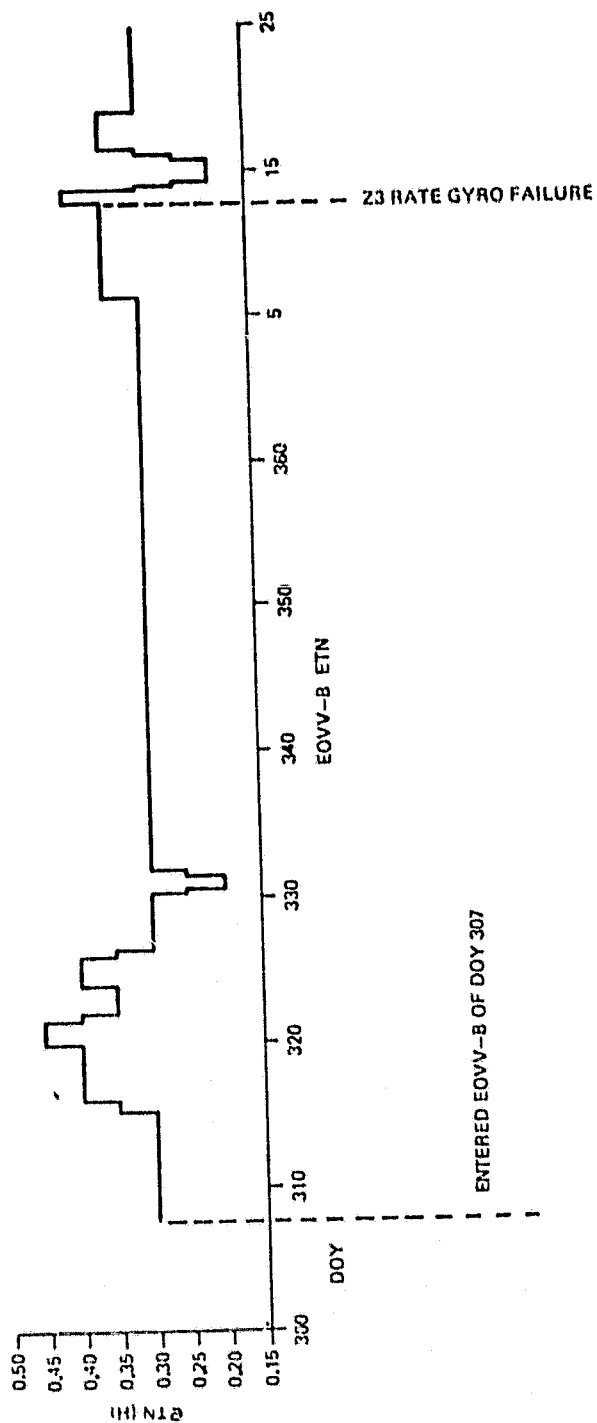
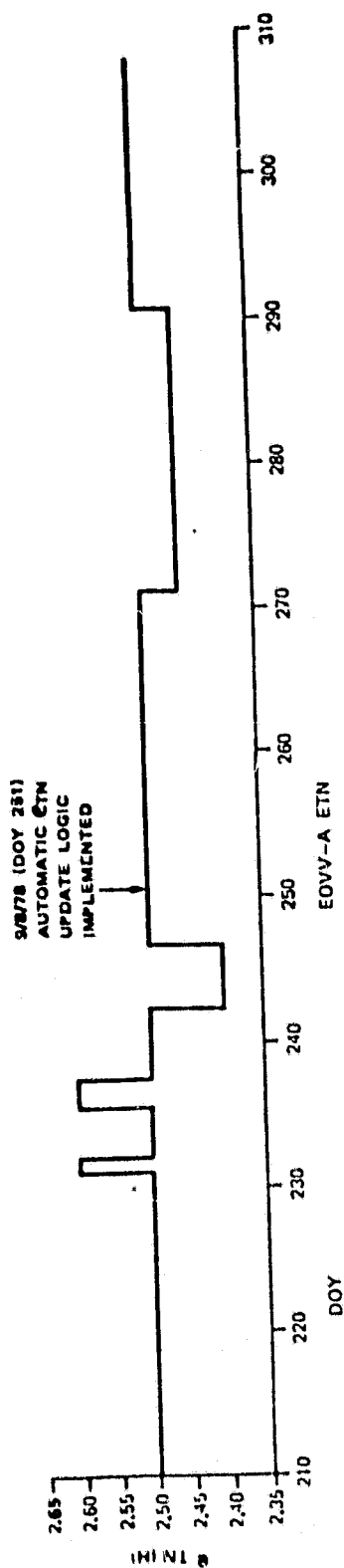


Figure 6. Orbital Y-momentum

in turn, could lead to large orbit plane misalignments to generate the required strapdown updates to keep up with the ± 50 deg rocking of the true orbital plane (due to the precession when viewed with respect to the projection of the sun-line into the orbital plane). The large size of the maximum change per orbit (1.2 deg) was not recognized at the beginning of the EOVV operation and was the cause for loss of attitude on June 28, 1978. After that the ideal strapdown update necessary to follow the rocking of the orbital plane was introduced open loop through the quantity called e_{rb} [equation. (12)] and no more problems were experienced (APPENDIX C).

APPENDIX A

COORDINATE SYSTEMS AND TRANSFORMATIONS

The coordinate systems which are pertinent to Skylab EOVV control are defined here. Each system has some special geometrical or physical feature which simplifies the solution of a particular problem.

The following coordinate systems are described: Principal, Orbital, Vehicle, Attitude Reference, Solar Inertial, and Z-Local Vertical. Each coordinate system consists of a set of mutually orthogonal axes exhibiting right-handedness.

An inertial (with respect to rotation only) coordinate system is a system which retains its orientation with respect to the celestial sphere, although the origin may be moving along any general curvilinear path in space. Similarly, a vehicle fixed system retains its orientation with respect to the vehicle.

Orbital Coordinate System (O)

The Orbital Coordinate System (x_o , y_o , z_o) is a precessing coordinate system with its origin at the Earth center of mass. The rate of precession about the Earth's north pole is approximately -5 degrees/day. The z_o axis lies in the orbital plane, positive through the ascending node of the orbit. The x_o axis also lies in the orbital plane 90 degrees ahead of the z_o axis. Since the Skylab orbit was in the $x_o z_o$ plane at all times, the y_o axis was parallel to the orbital angular momentum vector, completing the right-handed system (Fig. A-1).

Solar Inertial Coordinate System (I)

The Solar Inertial Coordinate System (x_I , y_I , z_I) is only a pseudo-inertial system since it makes one revolution per year. It was used during the Skylab mission to point the instruments in the desired direction. The origin is coincident with the origin of the Vehicle Coordinate System origin. The z_I axis is positive toward the center of the Sun. The x_I axis lies at an angle ψ_z from the orbital plane (this angle is calculated on-board such that the principal x axis is in the orbital plane to minimize the build-up of angular momentum) and is positive toward the sunset terminator.

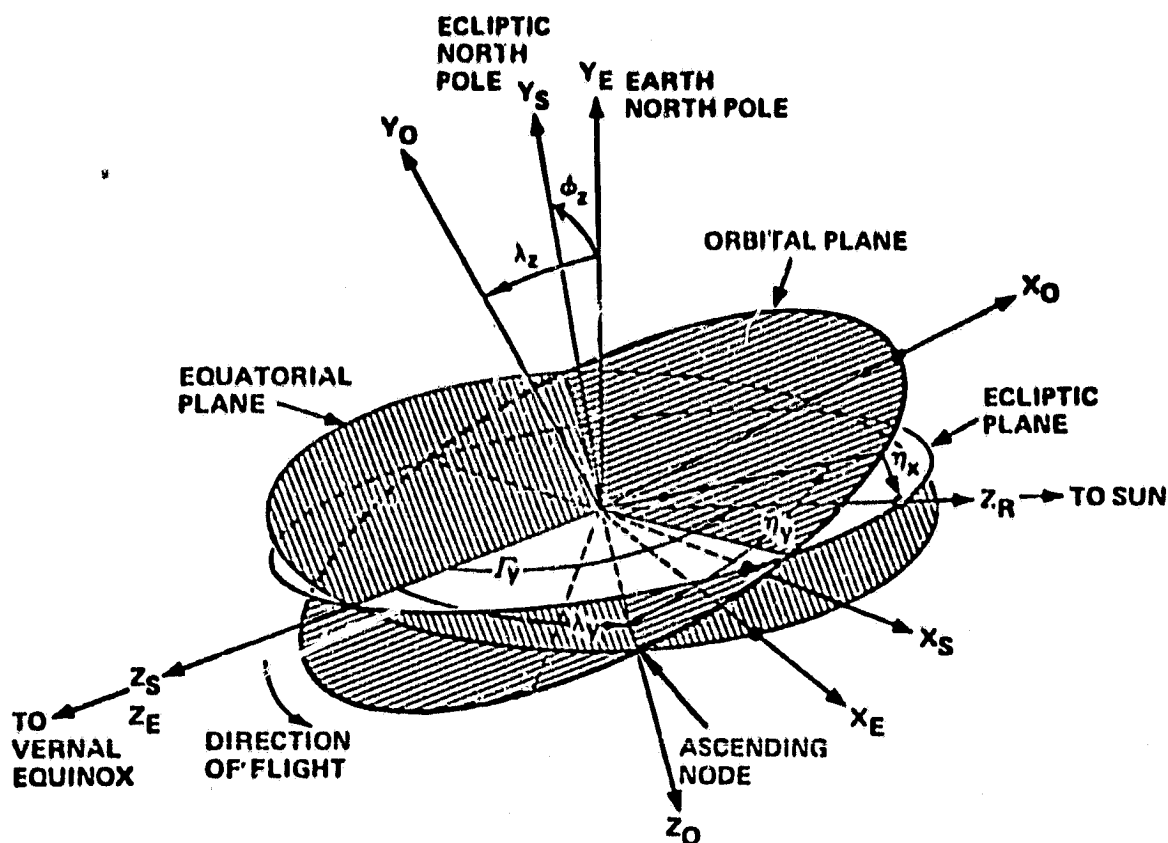


Figure A-1. Coordinate system.

Z-Local Vertical Coordinate System (L)

The z-Local Vertical Coordinate System (x_L, y_L, z_L) is a rotating system with its origin at the center of mass of Skylab (the rate of rotation is one revolution per orbit). The x_L axis is positive in the direction of flight and lies in the orbital plane. The z_L axis is parallel to the local vertical direction and is positive outward, away from the Earth. The y_L axis is parallel to the orbit normal and is positive toward orbital North.

Vehicle Coordinate System (V)

The Vehicle Coordinate System (x_V, y_V, z_V) is a vehicle-fixed system with its origin at the center of mass. The x_V axis lies along the long axis of Skylab and is positive in the direction of the Multiple Docking Adapter (MDA). The z_V axis is positive toward the Apollo Telescope Mount (ATM) and the y_V axis completes the right-handed system.

Principal Axes Coordinate System (P)

The Principal Axes Coordinate System (x_p, y_p, z_p) is a vehicle-fixed system with its origin at the center of mass. The axes are along the principal moment-of-inertia axes, labeled such that the eigen angle between the V and the P system is minimized.

The following transforms are useful (the subscripts 1, 2, 3 indicate rotation about x, y, z, respectively).

$$[LI] = [\Delta\eta_{ty}]_2 [-\eta_x]_1 [-v_{ZE}]_3$$

$$[AL] = [K]^T [\eta]_1 [\eta_z]_3 [\eta_y + \eta_{cy}]_2$$

$$[PV] = [K]$$

$$[VI] = \text{strapdown matrix (updated by } \underline{\omega}^V, \text{ sunsensor data and momentum data)}$$

APPENDIX B

GRAVITATIONAL TORQUE MODEL

The gravitational torques on a satellite produced by a large, spherical primary body are important contributors to its rotational dynamics. The force on a point mass m exerted by the primary M is

$$\underline{F}_i = - \frac{GMm}{|\underline{R}_i|^3} \underline{R}_i ; G = 6.672E-11 \text{ Nm}^2/\text{kg}^2 \quad . \quad (\text{B1})$$

The satellite can be viewed as a collection of point masses. The net torque on this collection of masses about the origin of satellite coordinates is

$$\underline{T}_g = - \sum_i \underline{r}_i \times \underline{F}_i \quad . \quad (\text{B2})$$

The vector \underline{r}_i is the position of m_i relative to the origin which is at \underline{R}_o relative to the primary center. Thus

$$\underline{R}_i = \underline{R}_o + \underline{r}_i \quad (\text{B3})$$

and

$$\underline{T}_g = - \sum_i \underline{r}_i \times GMm_i \frac{\underline{R}_o + \underline{r}_i}{|\underline{R}_o + \underline{r}_i|^3} \quad . \quad (\text{B4})$$

In general $|\underline{r}_i| \ll |\underline{R}_o|$ and hence an expansion of \underline{T}_g keeping only low order terms becomes sufficient for most purposes. Now

$$\frac{\underline{R}_o + \underline{r}_i}{|\underline{R}_o + \underline{r}_i|^3} = \frac{\underline{R}_o}{|\underline{R}_o|^3} + \frac{\underline{r}_i}{|\underline{R}_o|^3} - 3\underline{R}_o \frac{\underline{R}_o \cdot \underline{r}_i}{|\underline{R}_o|^5} + \text{h.o.t.} \quad (\text{B5})$$

Using the expansion of equation (B5) in (B4),

$$\underline{T}_g = - \underline{r}_{cm} \times \frac{GMm}{|\underline{R}_o|^3} \underline{R}_o + 3 \frac{GM}{|\underline{R}_o|^3} \sum_i m_i \underline{r}_i \times \underline{R}_o \frac{\underline{R}_o \cdot \underline{r}_i}{|\underline{R}_o|^3} + \text{h.o.t.} \quad (B6)$$

We have used the definition $m \underline{r}_{cm} = \sum_i m_i \underline{r}_i$. Rearranging and grouping equation (B6) we obtain

$$\underline{T}_g = - \underline{r}_{cm} \times \frac{GMm}{|\underline{R}_o|^3} \underline{R}_o + \frac{3GM}{|\underline{R}_o|^3} \frac{\underline{R}_o}{|\underline{R}_o|^3} \times \left(- \sum_i m_i \underline{r}_i \underline{r}_i \right) \cdot \frac{\underline{R}_o}{|\underline{R}_o|^3} + \text{h.o.t.} \quad (B7)$$

The term in parentheses in equation (B7) occurs in the definition of the moment of inertia dyadic (or tensor)

$$\underline{I} = \sum_i m_i (\underline{r}_i^2 \underline{1} - \underline{r}_i \underline{r}_i) \quad (B8)$$

Using this definition in equation (B7) and dropping the higher order terms yields the gravity gradient torque expression

$$\underline{T}_{gg} = - \underline{r}_{cm} \times \frac{GMm}{|\underline{R}_o|^3} \underline{R}_o + 3 \frac{GM}{|\underline{R}_o|^3} \frac{\underline{R}_o}{|\underline{R}_o|^3} \times \underline{I} \cdot \frac{\underline{R}_o}{|\underline{R}_o|^3} \quad (B9)$$

As can be seen, if the origin is positioned at the center of mass the more familiar gravity gradient torque expression results:

$$\underline{T}_{gg} = 3 \frac{GM}{|\underline{R}_O|^3} \frac{\underline{R}_O}{|\underline{R}_O|} \times \underline{I} \cdot \frac{\underline{R}_O}{|\underline{R}_O|} \quad (B10)$$

For an orbiting body m , the orbital angular velocity magnitude is given by

$$\Omega_O^2 = GM/|\underline{R}_O|^3 \quad (B11)$$

Noting that $\underline{R}_O/|\underline{R}_O|$ is a unit vector \underline{u}_R , we finally write

$$\underline{T}_{gg} = 3\Omega_O^2 \underline{u}_R \times \underline{I} \cdot \underline{u}_R \quad (B12)$$

The torque of equation (B12) is what is commonly referred to as the gravity gradient torque.

APPENDIX C.

STRAPDOWN DRIFT ERROR AND MOTION OF I COORDINATE SYSTEM

The basic reference coordinate system used during the original Skylab manned mission was the so-called Solar Inertial (I) coordinate system (Appendix A gives the definition). As stated there, I is not truly an inertial coordinate system since its axes rotate with the sun and orbit regression. Its rotation rate varies with the solar elevation angle out of the orbit plane. By definition, the z axis points toward the sun and the unit vector \underline{u}_{p1} lies in the orbit plane pointed generally parallel to the vehicle velocity vector at orbital noon. The unit vector \underline{u}_{p1} is the direction of the x principal axis in vehicle coordinates V. Thus, when the V and I systems are aligned, the vehicle x principal axis is in the orbit plane so that ideally all gravity gradient torques are cyclic. The sun angle Γ_y and orbit regression angle λ_y are updated once per orbit at orbit midnight in the Skylab navigation calculations. In between midnights, the I system, as defined by vehicle on-board navigation, does not rotate. As a consequence of this, it is useful to redefine I such that the definition given previously is only satisfied at midnight. Let I_k represent the true reference position (we use the convention that true or physical parameters are labelled by a subscript k) of this system and I represents the estimate. This estimate is made using the vehicle angular rates as measured by the rate gyros.

$$\underline{\omega}_{VI}^V = \underline{\omega}_{VIk}^V + \underline{\omega}_D^V .$$

The angular rates $\underline{\omega}_{VI}^V$, $\underline{\omega}_D^V$ and $\underline{\omega}_{VIk}^V$ are all given in the vehicle system V. The rate $\underline{\omega}_D^V$ is the gyro drift rate and experience indicates it tends to be constant in the vehicle system V. To a good approximation the vehicle remains fixed relative to the local vertical system L. Thus

$$\underline{\omega}_{VI}^V = \Omega_O \underline{u}_{L2}^V ,$$

where Ω_O is the orbital angular rate.

Since Ω_0 , u_{L2}^V and ω_D^V are constants, ω_{VIk}^V must also be constant

$$\omega_{VIk}^V = \Omega_0 u_{L2}^V - \omega_D^V .$$

We can integrate the rate ω_{VIk}^V using the differential equation

$$\frac{d}{dt} [VI_k] = - \omega_{VIk}^V [VI_k] .$$

This yields

$$[VI_k] = \exp \tilde{A} [VI_k]_0 ,$$

with

$$\exp \tilde{A} = \sum_{n=0}^{\infty} \frac{1}{n!} \tilde{A}^n = 1 - \sin |\underline{A}| \frac{\tilde{A}}{|\underline{A}|} + (1 - \cos |\underline{A}|) \frac{\tilde{A}\tilde{A}}{|\underline{A}|^2} ,$$

and

$$\underline{A} = - \omega_{VIk}^V T ,$$

where

$$T = 2\pi/\Omega_0 ,$$

is the orbital period.

Let $[VI_k]_0$ is the $[VI_k]$ transformation at the beginning of the orbit.

$$\underline{\theta} VI_k = \underline{\omega} VI_k T \quad ,$$

and

$$\underline{\theta}_D = \underline{\omega}_D T \quad ,$$

then

$$\underline{\theta} VI_k = 2\pi \underline{u}_{L2} - \underline{\theta}_D \quad .$$

We shall now assume that $|\underline{\theta}_D| \ll 2\pi$. In practice $|\underline{\theta}_D|$ is at most ~ 0.05 to 0.06 radians. Thus we can evaluate $\exp \left(-\underline{\theta} VI_k^V \right)$ keeping only 1st order terms in $\underline{\theta}_D^V$. First, we find

$$|\underline{\theta} VI_k| \approx 2\pi - \underline{u}_{L2} \cdot \underline{\theta}_D \quad .$$

Using this result, we find

$$\frac{\underline{\theta} VI_k}{|\underline{\theta} VI_k|} = \underline{u}_{L2} - \frac{1}{2\pi} (\underline{\theta}_D - \underline{\theta}_D \cdot \underline{u}_{L2} \underline{u}_{L2})$$

From this we find

$$\exp \left(-\underline{\theta} VI_k^V \right) = \exp \left(\underline{u}_{L2} \cdot \underline{\theta}_D \tilde{\underline{u}}_{L2}^V \right) \quad .$$

Finally

$$[VI_k] = \exp \left(\underline{\theta}_D \cdot \underline{u}_{L2} \tilde{\underline{u}}_{L2}^V \right) [VI_k]_0 \quad .$$

$$= [-\underline{0}_D \cdot \underline{u}_{L2}] \underline{u}_{L2}^V [VI_k]_0 \quad (C1)$$

$$\approx (1 + \underline{0}_D \cdot \underline{u}_{L2} \tilde{\underline{u}}_{L2}^V) [VI_k]_0$$

The result we have obtained in equation (C1) can be summarized by saying the strapdown error induced by gyro drift to the 1st approximation only accumulates along the orbit normal and tends to be purely cyclic along \underline{u}_{L1} and \underline{u}_{L3} .

Strapdown errors enter in also due to motion of the I coordinate system. These motions are not accounted for in the strapdown calculations and so must be corrected by updates from sun sensor data and momentum accumulation data as explained elsewhere. The solar inertial system motion is readily calculated from relative motion of the sun and from regression of the Skylab orbit. The sun moves approximately 1 deg per day while the orbit processes nearly 5.5 deg per day in the retrograde direction. Since there are about 16 orbits per day, these effects are usually small but occasionally amount to more than 1 deg per orbit. To analyze these effects let us define the system S such that the z axis points to the Vernal Equinox and y axis to the ecliptic north pole,

$$[SE] = [\phi_z]_3 = \begin{bmatrix} \cos\phi_z & \sin\phi_z & 0 \\ -\sin\phi_z & \cos\phi_z & 0 \\ 0 & 0 & 1 \end{bmatrix}; \quad \phi_z = 23.45^\circ$$

Also, define R such that z_R points to the sun and y_R to ecliptic north. From R to I is a rotation about z_R

$$[IR] = [\theta_z]_3$$

$$\rightarrow [IE] = [\theta_z]_3 [r_y]_2 [\phi_z]_3$$

where the numeric subscripts indicate the axis of the Euler angle rotation (1, 2, 3 represent x, y, z respectively).

The angular velocity of I relative to E is

$$\underline{\omega}_{IE}^I = \dot{\theta}_z \begin{bmatrix} 0 \\ 0 \\ 1 \end{bmatrix} + \dot{\Gamma}_y \begin{bmatrix} \sin \theta_z \\ \cos \theta_z \\ 0 \end{bmatrix} .$$

The transformation [IE] can also be computed from onboard navigation parameters

$$[IE] = [\nu_z]_3 [\eta_x]_1 [\eta_y]_2 [\lambda_z]_3 [\lambda_y]_2 . \quad (C2)$$

The angle λ_y is the orbit regression angle and $\dot{\lambda}_y$ is the nearly constant regression rate. The angles in equation (C2) can all be expressed in terms of λ_y and Γ_y . The vector \underline{u}_{P1} is a row from the vehicle-to-principal axes transformation [PV],

$$\underline{u}_{P1}^V = [PV]^T \begin{bmatrix} 1 \\ 0 \\ 0 \end{bmatrix} = \begin{bmatrix} PV_{11} \\ PV_{12} \\ PV_{13} \end{bmatrix} .$$

For convenience, we let $[K] = [PV]$ so that

$$\underline{u}_{P1}^V = \begin{bmatrix} K_{11} \\ K_{12} \\ K_{13} \end{bmatrix} .$$

The unit vector to the sun is \underline{u}_{R3} and is

$$\underline{u}_{R3}^E = \begin{bmatrix} \sin \Gamma_y \cos \phi_z \\ \sin \Gamma_y \sin \phi_z \\ \cos \Gamma_y \end{bmatrix} .$$

Similarly, the orbit normal is

$$\underline{u}_{O2}^E = \begin{bmatrix} -\sin\lambda_z \cos\lambda_y \\ \cos\lambda_z \\ \sin\lambda_z \sin\lambda_y \end{bmatrix} .$$

The angle η_y is by definition the position of orbital noon, i.e., the position in orbit where the radius vector, the solar vector, and the orbit normal are coplanar with $\underline{u}_{R3} \cdot \underline{u}_{L3} \geq 0$.

$$\eta_y = \tan^{-1} \left(\frac{\underline{u}_{R3x}^O}{\underline{u}_{R3z}^O} \right) ; \text{ where } \underline{u}_{R3}^O = [OE] \underline{u}_{R3}^E$$

$$[OE] = [\lambda_z]_3 [\lambda_y]_2$$

$$\eta_y = \tan^{-1} \left(\frac{\cos\lambda_z \cos\lambda_y \sin\Gamma_y \cos\phi_z + \sin\lambda_z \sin\Gamma_y \sin\phi_z - \cos\lambda_z \sin\lambda_y \cos\Gamma_y}{\sin\lambda_y \sin\Gamma_y \cos\phi_z + \cos\lambda_y \cos\Gamma_y} \right)$$

Note: The \tan^{-1} technique used must be a 4 quadrant technique! The angle η_x is the elevation angle of the sun out of the orbit plane with orbit south the positive hemisphere.

$$\eta_x = \sin^{-1} \underline{u}_{R3y}^O$$

$$= \sin^{-1} [\sin\lambda_z \cos\lambda_y \sin\Gamma_y \cos\phi_z - \cos\lambda_z \sin\Gamma_y \sin\phi_z - \sin\lambda_z \sin\lambda_y \cos\Gamma_y]$$

The remaining angle ν_z is obtained by solving

$$\underline{u}_{P1} \cdot \underline{u}_{O2} = 0 \text{ \& } \underline{u}_{P1} \cdot \underline{u}_{L1} \geq 0 \text{ at orbit noon} \quad (C3)$$

$$\rightarrow \nu_z = -\phi + \sin^{-1} \left(\frac{K_{13} \tan \eta_x}{\sqrt{1 - K_{13}^2}} \right); \phi = \tan^{-1} \left(\frac{K_{12}}{K_{11}} \right).$$

(4 Quadrant \tan^{-1})

With these intermediate angles and the values of λ_y , λ_z , Γ_y , ϕ_z , we can compute [IE] from equation (C2) for any time. We can also compute θ_z .

$$\underline{u}_{Oz}^{R'} = \begin{bmatrix} -\cos \Gamma_y \cos \phi_z \cos \lambda_y \sin \lambda_z + \cos \Gamma_y \cos \lambda_z \sin \phi_z - \sin \Gamma_y \sin \lambda_y \sin \lambda_z \\ \sin \phi_z \cos \lambda_y \sin \lambda_z + \cos \lambda_z \cos \phi_z \\ -\sin \Gamma_y \cos \phi_z \cos \lambda_y \sin \lambda_z + \sin \Gamma_y \cos \lambda_z \sin \phi_z + \cos \Gamma_y \sin \lambda_y \sin \lambda_z \end{bmatrix}$$

From equation (C4) then we obtain

$$\theta_z = -\sin^{-1} \frac{K_{13} u_{O2z}^R}{\sqrt{(1 - K_{13}^2)} (1 - u_{O2z}^R)} - \tan^{-1} \frac{K_{11} u_{O2x}^R + K_{12} u_{Ozy}^R}{K_{11} u_{O2y}^R - K_{12} u_{O2x}^R}.$$

We can now use equation (C1) to determine $\underline{\omega}_{IE}^I$. Figure C-1 shows how the components of $\underline{\omega}_{IE}^I$ vary with time as the sun elevation angle (the so-called β angle $\beta = -\eta_x$) goes through its maximum value in the northern orbital hemisphere. We had not realized prior to this that the solar inertial frame could move so fast and were unpleasantly surprised when EOVV attitude was lost due to strapdown drift and resultant momentum saturation. For more on this incident see Reference 2. After this incident, we developed a procedure to update the z momentum bias in such a way that the necessary rotations would be supplied by the bias value rather than a momentum error. The parameter was called a ramp bias, e_{rb} [equation (12)]. Since the z update angle depends on $e_r - e_{rb}$, we could keep e_r small by using e_{rb} and since we now knew what to expect we could plan in advance what e_{rb} updates were needed to keep e_r small. Table C-1 and Figure C-1 show the e_{rb} updates that should have been made to prevent the loss of momentum control we experienced. The knowledge and experience gained here allowed us to successfully pass through two similar peaks of opposite signs in November and January.

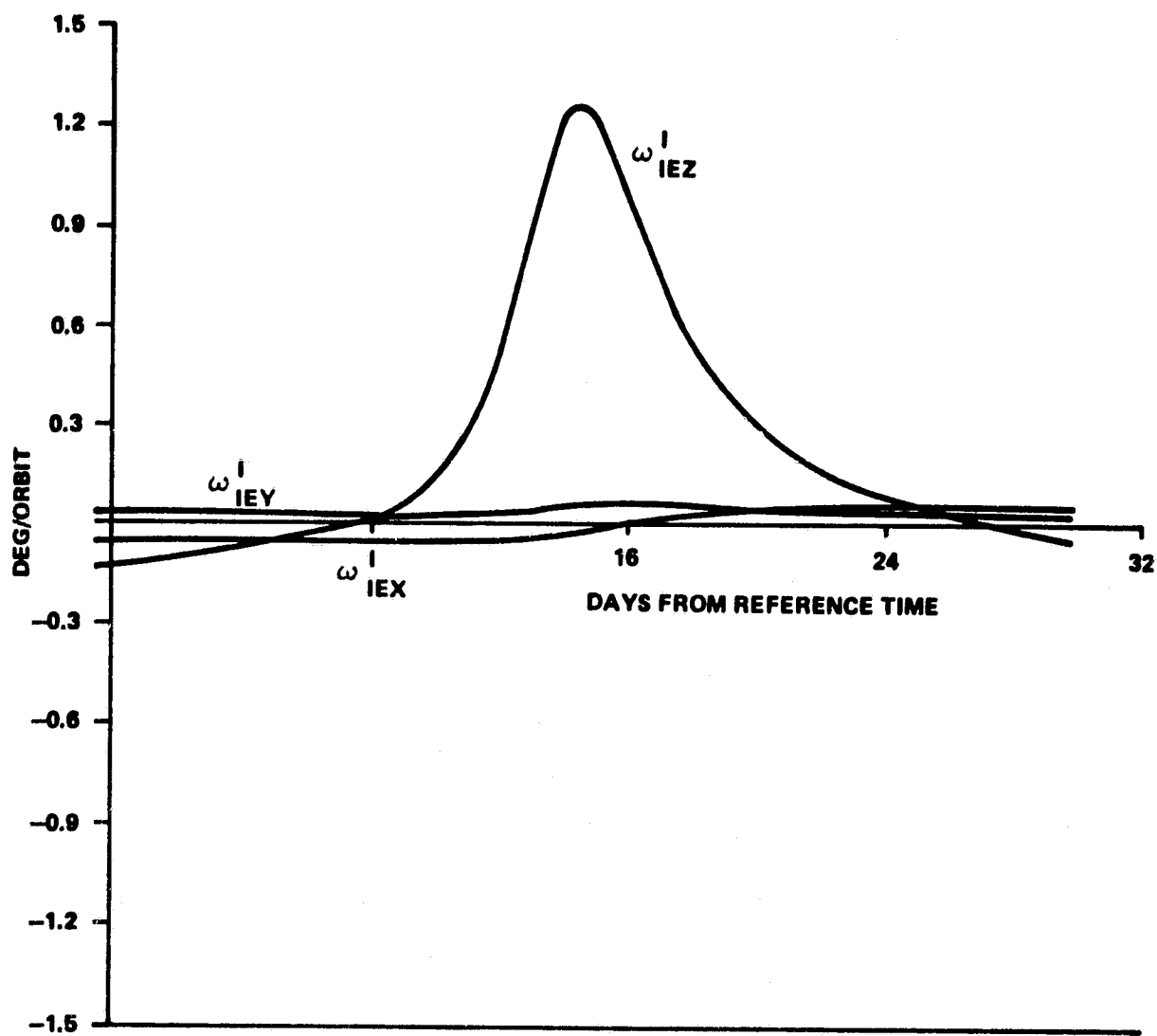


Figure C-1. Motion of I coordinate system (deg/orbit).

TABLE C-1. SCHEDULE OF ERB UPDATE TIMES

UPDATE TIME	NEW ERB VALUE IN LSBS		
166:18:0	2	181: 9:29	-23
170: 0:13	1	181:13:44	-22
172: 7:26	0	181:17:50	-21
173:16:13	-1	181:21:56	-20
174:13:27	-2	182: 2: 9	-19
175: 4: 7	-3	182: 6:29	-18
175:15:23	-4	182:10:49	-17
176: 0:34	-5	182:15:32	-16
176: 7:39	-6	182:20:23	-15
176:14: 3	-7	183: 1:26	-14
176:19:21	-8	183: 7: 2	-13
177: 0:30	-9	183:12:46	-12
177: 4:33	-10	183:19:20	-11
177: 8:35	-11	184: 2:16	-10
177:12:29	-12	184:10: 2	-9
177:15:41	-13	184:18:50	-8
177:18:52	-14	185: 4:44	-7
177:22: 4	-15	185:16: 9	-6
178: 1: 5	-16	186: 5:37	-5
178: 3:51	-17	186:21:42	-4
178: 6:36	-18	187:17:42	-3
178: 9:22	-19	188:18:53	-2
178:12: 6	-20	190: 3:27	-1
178:14:55	-21	191:21:33	0
178:17:43	-22	194: 0:48	1
178:20:30	-23		
178:23:18	-24		
179: 2:47	-25		
179: 6:30	-26		
179:10:13	-27		
179:16:36	-28		
180:13:18	-27		
180:19:11	-26		
181: 0:47	-25		
181: 6: 8	-24		

ASSUMES KNUZ IS 0.2

APPENDIX D. GAIN CALCULATIONS

a. Calculation of IOP Desaturation Gain $K_{\eta z}$

The local vertical in principal axes components is ($s = \sin$, $c = \cos$)

$$\underline{r}_p = \begin{bmatrix} cz & sz & 0 \\ -sz & cz & 0 \\ 0 & 0 & 1 \end{bmatrix} \begin{bmatrix} cy & 0 & -sy \\ 0 & 1 & 0 \\ sy & 0 & cy \end{bmatrix} \begin{bmatrix} 0 \\ 0 \\ 1 \end{bmatrix} = \begin{bmatrix} -czsy \\ szsy \\ cy \end{bmatrix},$$

where

$$y = \eta_{yn} = -\eta_{ym}s(2\Omega_0 t), \quad z = \eta_{zn} = -\eta_{zm}s(2\Omega_0 t),$$

and the η_{xn} rotation is neglected (a cylindrical inertia distribution is assumed with $I_y = I_z = I$ and $\Delta I = I - I_x$). The gravity gradient torque is (in P components)

$$\underline{T}_{ggp} = K_{gg} \begin{bmatrix} 0 \\ -r_1 & r_3 \\ r_1 & r_2 \end{bmatrix} = K_{gg} \begin{bmatrix} 0 \\ czsy \\ -czsysz \end{bmatrix},$$

where

$$K_{gg} = 3\Omega_0^2 \Delta I,$$

and in 0 components (where $Y = \Omega_0 t + y$)

$$\underline{T}_{ggo} = K_{gg} \begin{bmatrix} cY & 0 & sY \\ 0 & 1 & 0 \\ -sY & 0 & cY \end{bmatrix} \begin{bmatrix} cz & -sz & 0 \\ sz & cz & 0 \\ 0 & 0 & 1 \end{bmatrix} \begin{bmatrix} 0 \\ czsy \\ -szsysz \end{bmatrix}$$

$$= K_{gg} \text{ szczy } \begin{bmatrix} -c\Omega_0 t \\ cy/tz \\ s\Omega_0 t \end{bmatrix} .$$

For the further development only the IOP component is of interest, which is (assuming y and z small)

$$\underline{T}_{ggz,x} = K_{gg} \eta_{ym} \eta_{zm} s^2 (2\Omega_0 t) \begin{bmatrix} s\Omega_0 t \\ -c\Omega_0 t \end{bmatrix} .$$

Integrating over a quarter orbit yields

$$\begin{aligned} \underline{H}_{ggoz,x} &= 4 K_{gg} \eta_{ym} \eta_{zm} \int_0^{\pi/2\Omega_0} dt (s^2\Omega_0 t c^2\Omega_0 t) \begin{bmatrix} s\Omega_0 t \\ -c\Omega_0 t \end{bmatrix} \\ &= 4 K_{gg} \eta_{ym} \eta_{zm} \begin{bmatrix} \int_0^{\pi/2\Omega_0} dt s\Omega_0 t (c^2\Omega_0 t - c^4\Omega_0 t) \\ - \int_0^{\pi/2\Omega_0} dt c\Omega_0 t (s^2\Omega_0 t - s^4\Omega_0 t) \end{bmatrix} . \end{aligned}$$

Substitution yields

$$(u = c\Omega_0 t; v = s\Omega_0 t) ,$$

$$\underline{H}_{ggoz,x} = \frac{4}{\Omega_0} K_{gg} \eta_{ym} \eta_{zm} \begin{bmatrix} \int_0^1 du (u^2 - u^4) \\ - \int_0^1 dv (v^2 - v^4) \end{bmatrix} = \frac{4}{\Omega_0} K_{gg} \eta_{ym} \eta_{zm} \frac{2}{15} \begin{bmatrix} 1 \\ -1 \end{bmatrix} ,$$

$$\underline{H}_{\text{ggoz},x} = \frac{24}{15} \Omega_o \Delta I \eta_{ym} \eta_{zm} \begin{bmatrix} 1 \\ -1 \end{bmatrix} .$$

Rotation to the effective axis system yields

$$\underline{H}_{\text{ggz},x} = \frac{24}{15} \Omega_o \Delta I \eta_{ym} \eta_{zm} \frac{1}{\sqrt{2}} \begin{bmatrix} 1 & 1 \\ -1 & 1 \end{bmatrix} \begin{bmatrix} 1 \\ -1 \end{bmatrix} ,$$

$$H_{\text{ggz}} = 0 ,$$

$$H_{\text{ggx}} = - (24 \sqrt{2}/15) \Omega \Delta I \eta_{ym} \eta_{zm} .$$

Resolving actual momentum to be desaturated into the same axes

$$\frac{1}{\sqrt{2}} \begin{bmatrix} H_z + H_x \\ -H_z + H_x \end{bmatrix} = \frac{1}{\sqrt{2}} \begin{bmatrix} 1 & 1 \\ -1 & 1 \end{bmatrix} \begin{bmatrix} H_z \\ H_x \end{bmatrix} .$$

Only the x component can be desaturated leading to (in units of the nominal angular momentum H of one CMG):

$$(H/\sqrt{2}) (e_x - e_z) = (48/15\sqrt{2}) \Omega_o \Delta I \eta_{ym} \eta_{zm} ,$$

or

$$\eta_{zm} = K_{\eta z} (e_x - e_z) ,$$

with the gain being

$$K_{\eta z} = (15H)/(48\Omega_o \Delta I \eta_{ym}) .$$

b. Calculation of POP Gain K_{yc}

The gravity gradient orbital y torque for a rotation η_y about the orbital y axis through η_y is (APPENDIX B)

$$T_{ggoy} = K_{gg} s\eta_y c\eta_y$$

$$\approx K_{gg} \eta_y$$

If the angle η_y is held constant over the desaturation period T_{des} (about 1/12 of an orbit) we get an orbital y momentum change of

$$\Delta e_{ggoy} = K_{gg} T_{des} \eta_y / H$$

in units of the nominal CMG momentum H. For a given Δe_{oy} we need

$$\eta_{yc} = K_{yc} \Delta e_{oy}$$

with

$$K_{yc} = H / (3\Omega_o^2 \Delta T_{des})$$

c. Calculation of Strapdown Update Gain $K_{\mu z}$

The components of the local vertical in the P system are (neglecting the tilt angle η_{zm} ; $s = \sin$, $c = \cos$)

$$\underline{r}_p = \begin{bmatrix} cN & 0 & -sN \\ 0 & 1 & 0 \\ sN & 0 & cN \end{bmatrix} \begin{bmatrix} 1 & z & 0 \\ -z & 1 & 0 \\ 0 & 0 & 1 \end{bmatrix} \begin{bmatrix} cy & 0 & sy \\ 0 & 1 & 0 \\ -sy & 0 & cy \end{bmatrix} \begin{bmatrix} 0 \\ 0 \\ 1 \end{bmatrix} = \begin{bmatrix} -sn \\ -zsy \\ cn \end{bmatrix}$$

with

$$N = y + n; y = \Omega_0 t; n = -\eta_{ym} s(2\Omega_0 t); s\mu_z \approx z; c\mu_z \approx 1.$$

For $I = I_y = I_z$ and $\Delta I = I - I_x$ we get for the principal axis torque due to the gravity gradient in the inertially fixed O system (with $K_{gg} = 3\Omega_0^2 \Delta I$)

$$\underline{T}_{gg} = K_{gg} r_1 \begin{bmatrix} cN & 0 & sN \\ 0 & 1 & 0 \\ -sN & 0 & cN \end{bmatrix} \begin{bmatrix} 0 \\ -r_3 \\ r_2 \end{bmatrix} = K_{gg} r_1 \begin{bmatrix} r_2 sN \\ -r_3 \\ r_2 cN \end{bmatrix}.$$

Only the torque about the z axis is of interest

$$T_{ggz} = K_{gg} z s n s y (c y e n - s y s n).$$

With $n = K s 2 y$; $s n \approx K s 2 y$; $c n \approx 1$ and $K = -\eta_{ym}$ we get

$$\begin{aligned} T_{ggz} &= K_{gg} z K s 2 y s y (c y - s y K s 2 y) \\ &= 0.25 K_{gg} z K [(1 - K) - (1 - K) c 4 y - 2 y c 4 y]. \end{aligned}$$

Elimination of the cyclic terms leaves a constant bias torque of

$$T_{ggz} = 0.25 K_{gg} z K (1 - K).$$

Integrating over an orbit ($T_{orbit} = 2\pi/\Omega_0$) and substituting the value for z , K_{gg} , and K gives

$$\Delta H_{ggz bias} = - (3/2) \Omega_0 \Delta I \eta_{ym} (1 + \eta_{ym}).$$

Inversion yields

$$\mu_z = - K_{\mu z} e_{zr} ,$$

where

$$K_{\mu z} = 2H/[3\Omega_o \Delta I \eta_{ym} (1 + \eta_{ym})] ,$$

and e_{zr} is the normalized z momentum ramp.

Because of noise, a much smaller $K_{\mu z}$ value had to be used in actual operation (see EOVS OPERATION and PERFORMANCE).

APPENDIX E

QUATERNIONS - A BRIEF EXPOSITION

Complex numbers of the form $z = a + ib$ have proven to be a valuable concept in the study of many physical phenomena. A generalization of this concept which proves useful in the study of rotational motion is the quaternion. Recall that the imaginary unit $i = \sqrt{-1}$. Let us define additional units j and k together with the product operation \circ :

$$i \circ i = j \circ j = k \circ k = -1$$

$$i \circ j = -j \circ i = k$$

(E1)

$$j \circ k = -k \circ j = i$$

$$k \circ i = -i \circ k = j$$

We shall define a quaternion as any quantity of the form

$$Q = Q_4 + i Q_1 + j Q_2 + k Q_3 \quad , \quad (E2)$$

(See Note 1 at end of Appendix E.) By analogy to the complex number terminology Q_4 is referred to as the real or scalar part of Q . It will also be convenient to think of the remaining part of Q as the imaginary or vector part. The reason for this will become clear as we proceed. Let $R = R_4 + iR_1 + jR_2 + kR_3$. The sum of quaternions Q and R is defined as

$$\begin{aligned} S = Q + R &= (Q_4 + R_4) + i (Q_1 + R_1) \\ &\quad + j (Q_2 + R_2) + k (Q_3 + R_3) \quad . \end{aligned} \quad (E3)$$

From this definition we can see that the sum operation is commutative and associative. We can now give the complete definition of the product operation \circ :

$$\begin{aligned}
P = Q \circ R = & (Q_4 R_4 - Q_1 R_1 - Q_2 R_2 - Q_3 R_3) \\
& + i (Q_4 R_1 + Q_1 R_4 + Q_2 R_3 - Q_3 R_2) \\
& + j (Q_4 R_2 + Q_2 R_4 + Q_3 R_1 - Q_1 R_3) \\
& + k (Q_4 R_3 + Q_3 R_4 + Q_1 R_2 - Q_2 R_1) \quad . \quad (E4)
\end{aligned}$$

With this definition we can show that \circ is associative and distributive but not commutative, i.e., $Q \circ R \neq R \circ Q$. We shall call any quaternion having zero imaginary part a scalar and, obviously, the algebra of scalars is just the algebra of real numbers. Thus, multiplication of a quaternion by a scalar simply results in a quaternion whose elements are multiplied by that scalar according to definition E4. We can now define the difference operation as

$$D = Q - R = Q + (-1) \circ R \quad . \quad (E5)$$

For convenience, we shall always omit the \circ when multiplying a quaternion by a scalar so that $(-2) \circ Q = -2 Q$.

By analogy to complex algebra, let us define the conjugate quaternion to Q . The conjugation operation will be denoted by $()^*$. Thus

$$Q^* = Q_4 - i Q_1 - j Q_2 - k Q_3 \quad . \quad (E6)$$

So far all of our definitions have been extensions of those for complex numbers as can be seen by assuming $Q_2 = Q_3 = R_2 = R_3 = 0$. Thus the complex number system is a subset of the quaternions. It can be easily seen that

$$Q^* \circ Q = Q \circ Q^* = Q_1 Q_1 + Q_2 Q_2 + Q_3 Q_3 + Q_4 Q_4 \quad , \quad (E7)$$

Note that $Q^* \circ Q$ is a pure real number or scalar. With this observation we can define the inverse:

$$Q^{-1} = (1/(Q^* \circ Q)) Q^* = Q^*/(Q^* \circ Q) ; Q^* \circ Q \neq 0 \quad . \quad (E8)$$

Finally then, we can define a division operation:

$$Q : R = Q \circ R^{-1} \quad . \quad (E9)$$

We can see that $Q : Q = Q \circ Q^{-1} = Q^{-1} \circ Q = 1$ so that Q^{-1} satisfies the necessary properties of an inverse as long as $Q \neq 0$. This will be useful later.

We need some additional results and definitions. First we can show that

$$(Q \circ R)^* = R^* \circ Q^* \quad . \quad (E10)$$

If the quaternion $Q = Q^*$, then Q is necessarily a scalar. Also, if $Q = -Q^*$, Q is purely imaginary or a vector quaternion. If V is a vector quaternion, we shall designate this by an underline as is also used to designate a 3-space vector, i.e., (i , j , and k will not be underlined)

$$\underline{V} = i V_1 + j V_2 + k V_3 \quad . \quad (E11)$$

For compactness of our notation we shall let

$$Q = Q_4 + \underline{Q} \quad , \quad (E12)$$

where

$$\underline{Q} = i Q_1 + j Q_2 + k Q_3.$$

Thus

$$Q \circ R = (Q_4 R_4 - \underline{Q} \cdot \underline{R}) + Q_4 \underline{R} + R_4 \underline{Q} + \underline{Q} \times \underline{R} \quad . \quad (E13)$$

The operations \cdot and \times are defined as for 3-space vectors so that

$$\underline{Q} \cdot \underline{R} = Q_1 R_1 + Q_2 R_2 + Q_3 R_3 \quad (E14)$$

and

$$\begin{aligned} \underline{Q} \times \underline{R} = & i (Q_2 R_3 - Q_3 R_2) + j (Q_3 R_1 - Q_1 R_3) \\ & + k (Q_1 R_3 - Q_3 R_1) \end{aligned} \quad (E15)$$

For vectors \underline{A} and \underline{B} ,

$$\underline{A} \circ \underline{B} = -\underline{A} \cdot \underline{B} + \underline{A} \times \underline{B} \quad (E16)$$

In general the product of quaternions mixes scalar and vector parts together so that this product is not very interesting in the study of rotational motion in 3-space. The triple product

$$\underline{V}' = \underline{Q}^* \circ \underline{V} \circ \underline{Q} \quad (E17)$$

is more interesting since it does preserve scalar and vector parts of \underline{V} without mixing them. This property is trivial for the scalar part of \underline{V} and follows for the vector part since

$$\underline{V}'^* = (\underline{Q}^* \circ \underline{V} \circ \underline{Q})^* = -\underline{Q}^* \circ \underline{V} \circ \underline{Q} = -\underline{V}' \quad (E18)$$

Hence as noted the triple quaternion product (E17) takes a scalar into a scalar and a vector into a vector for any quaternion \underline{Q} . Furthermore, the length of the vector $|\underline{V}| = \sqrt{\underline{V} \cdot \underline{V}}$ and

$$\begin{aligned} \underline{V}' \cdot \underline{V}' &= \underline{V}' \circ \underline{V}'^* = \underline{Q}^* \circ \underline{V} \circ \underline{Q} \circ (\underline{Q}^* \circ \underline{V} \circ \underline{Q})^* \\ &= (\underline{Q}^* \circ \underline{Q})^2 \underline{V} \circ \underline{V}^* \end{aligned} \quad (E19)$$

Equation (E19) indicates the triple product (E17) multiplies vector length by the factor $\underline{Q}^* \circ \underline{Q}$ which is a real number. We note that if $\underline{Q}^* \circ \underline{Q} = 1$, vector length is preserved and the vector mapping $\underline{V} \rightarrow \underline{V}'$ looks like a rotation operator. It is a linear operator in that $\underline{a}\underline{A} + \underline{b}\underline{B} \rightarrow \underline{a}\underline{A}' + \underline{b}\underline{B}'$. Restricting ourselves to normalized quaternions which preserve length, we see that E17 is equivalent to a rotation of vector \underline{V} into \underline{V}' . Since we are looking only at normalized quaternions, we can without loss of generality, represent \underline{Q} as

$$\underline{Q} = \cos \phi/2 + \sin \phi/2 \underline{u} \quad ; \quad \text{where } \underline{u} \cdot \underline{u} = 1 \quad . \quad (\text{E20})$$

The triple product equation (E17) can be combined with equation (E20) to give

$$\underline{V}' = \cos \phi \underline{V} - \sin \phi \underline{u} \times \underline{V} + (1 - \cos \phi) \underline{u} \underline{u} \cdot \underline{V} \quad . \quad (\text{E21})$$

Equation (E21) is the general form of the rotation of a vector \underline{V} about axis \underline{u} through the angle $-\phi$. That this is true is seen by examining the rotation operation. Clearly any vector along the rotation axis \underline{u} is not changed by the rotation so that if the vector \underline{V} is broken into parts parallel to and normal to \underline{u} ; i.e.

$$\underline{V} = \underline{V}_{\parallel} + \underline{V}_{\perp} \quad , \quad \text{where } \underline{V}_{\parallel} = \underline{V} \cdot \underline{u} \underline{u} \text{ and } \underline{V}_{\perp} \cdot \underline{u} = 0 \quad . \quad (\text{E22})$$

We must also have $\underline{V}' = \underline{V}_{\parallel} + \underline{V}'_{\perp}$; where $\underline{V}'_{\perp} \cdot \underline{u} = 0$ and $\underline{V}_{\parallel} = \underline{V}'_{\parallel}$. Since \underline{V}_{\perp} and \underline{V}'_{\perp} are normal to \underline{u} , we can express \underline{V}'_{\perp} as

$$\underline{V}'_{\perp} = x \underline{u} \times \underline{V}_{\perp} + y \underline{u} \times (\underline{u} \times \underline{V}_{\perp}) \quad . \quad (\text{E23})$$

Now $\underline{V}'_{\perp} \cdot \underline{V}_{\perp} = |\underline{V}_{\perp}|^2 \cos \alpha = -y |\underline{V}_{\perp}|^2 \rightarrow y = -\cos \alpha$ and $\underline{V}_{\perp} \times \underline{V}'_{\perp} = |\underline{V}_{\perp}|^2 \sin \alpha \underline{u}$ and thus $x = \sin \alpha$; where α is the rotation angle. Combining, we obtain

$$\underline{V}'_{\perp} = \sin \alpha \underline{u} \times \underline{V}_{\perp} - \cos \alpha \underline{u} \times (\underline{u} \times \underline{V}_{\perp}) \quad (\text{E24})$$

and

$$\underline{V}' = \underline{u} \underline{u} \cdot \underline{V} + \sin \alpha \underline{u} \times \underline{V} - \cos \alpha \underline{u} \times (\underline{u} \times \underline{V}) \quad . \quad (\text{E25})$$

The equivalence between equations (E21) and (E25) for $\alpha = -\phi$ is established. Thus, the mapping (E17) is equivalent to a rotation operator in a vector 3-space. Since the coordinate directions are also vectors, we can rotate the coordinate system instead of the vector. Rotating the vector through $-\phi$ yields the same components \underline{V}' as rotating the coordinate axes through ϕ . Thus we can look at \underline{V}' as a new vector formed from \underline{V} by rotation and expressed in the old axis system or as the old

vector expressed in new axes rotated relative to the old. We have now demonstrated that any coordinate system rotation can be represented by a quaternion. Note that if Q satisfies equation (E17), then so does $-Q$. Looking back at equation (E20) tells us that $-Q$ corresponds to $\phi + 360$ degrees which represents the same attitude ϕ does.

We now look at the time variations of Q . Since Q is constrained to be normalized, we necessarily have

$$d/dt(Q^* \circ Q) = 0 = \dot{Q}^* \circ Q + Q^* \circ \dot{Q} \quad . \quad (E26)$$

We see from equation (E26) that $Q^* \circ \dot{Q} = -(\dot{Q}^* \circ Q)^*$ and hence must be a vector. Let us define this vector by

$$Q^* \circ \dot{Q} = 1/2 \underline{\omega} \quad (E27)$$

$$\rightarrow \dot{Q} = 1/2 Q \circ \underline{\omega} \quad (\text{since } Q \circ Q^* = Q^* \circ Q = 1) \quad . \quad (E28)$$

We shall see the reason for the $1/2$ factor later. When we evaluate the rate of change of a vector with time in two reference frames, we find

$$\dot{\underline{V}} = Q \circ \dot{\underline{V}}' \circ Q^* + \dot{Q} \circ \underline{V}' \circ Q^* + Q \circ \underline{V}' \circ \dot{Q}^* \quad . \quad (E29)$$

Using equations (E28) in (E29),

$$\dot{\underline{V}} = Q \circ [\dot{\underline{V}}' + 1/2 (\underline{\omega} \circ \underline{V}' - \underline{V}' \circ \underline{\omega})] \circ Q^* \quad (E30)$$

$$\dot{\underline{V}} = Q \circ [\dot{\underline{V}}' + \underline{\omega} \times \underline{V}'] \circ Q^* \quad . \quad (E31)$$

Now the reason for the factor $1/2$ becomes clear. It is so that we can identify $\underline{\omega}$. Equation (E31) is exactly like the corresponding equation for 3-space vectors if we identify $\underline{\omega}$ as the angular velocity of the primed reference frame expressed in primed coordinates. This identification follows from the fact that equation (E31) holds for an arbitrary vector \underline{V} . Thus, $\underline{\omega}$ is identified as the relative angular velocity of the primed axes with respect to the unprimed.

The above discussion completes the basic development of our quaternion tools. We now turn to the problem of developing a more convenient notation. The most logical choice which comes to mind is a matrix representation. The quaternion Q would logically become

$$Q = \begin{bmatrix} Q1 \\ Q2 \\ Q3 \\ Q4 \end{bmatrix} . \quad (E32)$$

Looking back to the definition equation (E4) of the quaternion product \circ , we see that for $P = Q \circ R$ we have

$$P = \begin{bmatrix} Q4 & -Q3 & Q2 & Q1 \\ Q3 & Q4 & -Q1 & Q2 \\ -Q2 & Q1 & Q4 & Q3 \\ -Q1 & -Q2 & -Q3 & Q4 \end{bmatrix} \begin{bmatrix} R1 \\ R2 \\ R3 \\ R4 \end{bmatrix} \triangleq \tilde{Q} R . \quad (E33)$$

(See Notes at end of Appendix E.) Similarly, if $D = A \circ B \circ C$, then

$$D = A \circ B \circ C = \widetilde{\widetilde{A}} B C = \tilde{A} \tilde{B} C . \quad (E34)$$

This result shows that the set of matrices of the form \tilde{Q} have the properties of the quaternions and in fact comprise a matrix representation of quaternion algebra with matrix multiplication corresponding to \circ . We can also express the quaternion product in the alternate form

$$P = \begin{bmatrix} R4 & R3 & -R2 & R1 \\ -R3 & R4 & R1 & R2 \\ R2 & -R1 & R4 & R3 \\ -R1 & -R2 & -R3 & R4 \end{bmatrix} \begin{bmatrix} Q1 \\ Q2 \\ Q3 \\ Q4 \end{bmatrix} \triangleq \overline{\overline{R}} Q \quad (E35)$$

(See Notes at end of Appendix E.) Here the mapping also yields a matrix representation except the order of the factors must be reversed. Thus, we have

$$P = \tilde{Q} R = \tilde{R} Q$$

$$D = \tilde{A} \tilde{B} C = \tilde{C} \tilde{B} A \quad . \quad (E36)$$

$$\overline{\overline{B} \circ \overline{C}} = \tilde{C} \tilde{B}$$

According to these definitions and results, we have

$$\tilde{A} \tilde{B} C = \tilde{A} \tilde{C} B = \tilde{C} \tilde{B} A = \tilde{C} \tilde{A} B \quad . \quad (E37)$$

Thus, an interesting and sometimes useful result is that $\tilde{A} \tilde{C} = \tilde{C} \tilde{A}$. Let us now look at our previous work and make use of these new definitions:

$$\underline{V}' = Q^* \circ \underline{V} \circ Q \rightarrow \underline{V}' = \tilde{Q}^* \tilde{V} Q = \tilde{Q}^* \tilde{Q} \underline{V} \quad . \quad (E38)$$

Note that we now have a matrix formed from Q which rotates coordinate axes and produces \underline{V}' from \underline{V} . Linear vector spaces are also represented by matrices. The 3-space vectors, \underline{V} and \underline{V}' are related as

$$\underline{V}' = M \underline{V} \quad . \quad (E39)$$

Here M is a 3×3 matrix which transforms components of \underline{V} to primed coordinates. Referring back to equation (E25) and replacing α by $-\phi$ we see that

$$M = \underline{u} \underline{u}^T - \sin \phi \tilde{u} + \cos \phi (\mathbb{I} - \underline{u} \underline{u}^T) \quad . \quad (E40)$$

(See Notes at end of Appendix E.) The matrix \tilde{u} is the so-called cross product matrix and just happens to be the upper 3×3 formed by dropping the final row and column of $\tilde{\tilde{u}}$. The matrix \mathbb{I} is the identity matrix of the appropriate size to fit the current application. We have already shown the equivalence between M and $\tilde{Q}^* \tilde{Q}$. Let us look more closely at the latter since it is 4×4 . We can partition the double-tilde or double-bar matrices as

$$\tilde{Q} = Q_4 \mathbf{1} + \left[\begin{array}{c|c} Q & \underline{Q} \\ \hline -Q^T & 0 \end{array} \right] ; \quad \bar{Q} = Q_4 \mathbf{1} + \left[\begin{array}{c|c} -\tilde{Q} & \underline{Q} \\ \hline -\underline{Q}^T & 0 \end{array} \right] \quad (E41)$$

Since $Q^* \circ Q = \mathbf{1}$, $Q^* = Q^{-1}$ so that $Q^* Q = \mathbf{1}$. Also, $Q^* = Q$ (transpose) so that

$$\tilde{Q}^* \bar{Q} = \left[\begin{array}{c|c} Q_4^2 \mathbf{1} - 2 Q_4 \tilde{Q} + \tilde{Q} \tilde{Q} + \underline{Q} \underline{Q}^T & 0 \\ \hline 0 & 1 \end{array} \right] \quad (E42)$$

Hence $M = Q_4^2 \mathbf{1} - 2 Q_4 \tilde{Q} + 2 \underline{Q} \underline{Q}^T - Q^2 \mathbf{1}$. In expanded form

$$M = \left[\begin{array}{c|c|c} Q_1^2 - Q_2^2 - Q_3^2 + Q_4^2 & 2(Q_1 Q_2 + Q_3 Q_4) & 2(Q_1 Q_3 - Q_2 Q_4) \\ 2(Q_2 Q_1 - Q_3 Q_4) & -Q_1^2 + Q_2^2 - Q_3^2 + Q_4^2 & 2(Q_2 Q_3 + Q_1 Q_4) \\ 2(Q_3 Q_1 + Q_2 Q_4) & 2(Q_3 Q_2 - Q_1 Q_4) & Q_1^2 - Q_2^2 + Q_3^2 + Q_4^2 \end{array} \right] \quad (E43)$$

From equation (E28)

$$\dot{Q} = \frac{1}{2} Q \circ \underline{\omega} = \frac{1}{2} \underline{\omega} Q = \frac{1}{2} \left[\begin{array}{cccc} 0 & \omega_3 & -\omega_2 & \omega_1 \\ -\omega_3 & 0 & \omega_1 & \omega_2 \\ \omega_2 & -\omega_1 & 0 & \omega_3 \\ -\omega_1 & -\omega_2 & -\omega_3 & 0 \end{array} \right] \left[\begin{array}{c} Q_1 \\ Q_2 \\ Q_3 \\ Q_4 \end{array} \right] \quad (E44)$$

Equations (E43) and (E44) summarize the useful results from our discussion.

We are now ready to consider the question of successive rotations applied to a coordinate reference. A coordinate frame rotation is a rigid displacement of all the points in the system with a fixed axis passing through the origin. Thus, it would seem that several successive rotations should displace every point except the origin. Let us now consider the coordinate frame as a rigid body and determine the most general displacement of it which keeps one point fixed. We must first explain what is

meant by a rigid body displacement. A rigid body displacement is one which preserves distances between every possible pair of points in the body. The displacement is mathematically represented as a vector function \underline{f} . This function then has two basic properties:

$$1) \quad \underline{f}(0) = 0$$

$$2) \quad |\underline{f}(\underline{r}_A) - \underline{f}(\underline{r}_B)| = |\underline{r}_A - \underline{r}_B| \quad . \quad (E45)$$

To study this in more detail, we define two additional points \underline{r}_1 and \underline{r}_2 together with their images under \underline{f} , $\underline{f}(\underline{r}_1)$ and $\underline{f}(\underline{r}_2)$. Let $\underline{f}_1 = \underline{f}(\underline{r}_1)$ and $\underline{f}_2 = \underline{f}(\underline{r}_2)$. Let us define unit vectors

$$\underline{i} = \underline{r}_1 / |\underline{r}_1| \quad ; \quad \underline{u}_1 = \underline{f}_1 / |\underline{f}_1| \quad (E46)$$

$$\underline{j} = \frac{\underline{r}_2 - \underline{r}_2 \cdot \underline{i} \underline{i}}{|\underline{r}_2 - \underline{r}_2 \cdot \underline{i} \underline{i}|} \quad ; \quad \underline{u}_2 = \frac{\underline{f}_2 - \underline{f}_2 \cdot \underline{u}_1 \underline{u}_1}{|\underline{f}_2 - \underline{f}_2 \cdot \underline{u}_1 \underline{u}_1|} \quad .$$

$$\underline{k} = \underline{i} \times \underline{j} \quad ; \quad \underline{u}_3 = \underline{u}_1 \times \underline{u}_2$$

The vectors \underline{i} , \underline{j} , \underline{k} and \underline{u}_1 , \underline{u}_2 , \underline{u}_3 each form orthonormal bases for 3 dimensional space. An arbitrary vector \underline{r} can be expressed as

$$\underline{r} = x \underline{i} + y \underline{j} + z \underline{k} \quad . \quad (E47)$$

The corresponding $\underline{f}(\underline{r}) = f_x \underline{u}_1 + f_y \underline{u}_2 + f_z \underline{u}_3$. Condition 2 of equation (E45) can only be satisfied if

$$\underline{f}(\underline{r}) = x \underline{u}_1 + y \underline{u}_2 \pm z \underline{u}_3 \quad . \quad (E48)$$

Thus we can define two functions \underline{f}_+ and \underline{f}_- that both satisfy equation (E45) and map \underline{r}_1 into \underline{f}_1 and \underline{r}_2 into \underline{f}_2 . The function \underline{f}_- can be viewed as the reflection $(x, y, z) \rightarrow (x, y, -z)$ followed by \underline{f}_+ . We are only

interested in continuous transitions from an initial position to a final position and thus reflections must be eliminated since it is not possible to go from (x, y, z) to $(x, y, -z)$ continuously without violating condition 2 of equation (E45). Thus continuous rigid displacements can only occur in the form $\underline{f}+$. This function can be written out as

$$\underline{f}(\underline{r}) = x \underline{u}_1 + y \underline{u}_2 + z \underline{u}_3 = \alpha_x \underline{i} + \alpha_y \underline{j} + \alpha_z \underline{k} \quad (\text{E49})$$

$$\alpha_x = x \underline{u}_1 \cdot \underline{i} + y \underline{u}_2 \cdot \underline{i} + z \underline{u}_3 \cdot \underline{i}$$

$$\alpha_y = x \underline{u}_1 \cdot \underline{j} + y \underline{u}_2 \cdot \underline{j} + z \underline{u}_3 \cdot \underline{j} \quad (\text{E50})$$

$$\alpha_z = x \underline{u}_1 \cdot \underline{k} + y \underline{u}_2 \cdot \underline{k} + z \underline{u}_3 \cdot \underline{k} \quad .$$

Equation (E50) can be rewritten in the matrix form

$$\underline{\alpha} = M \underline{r} \quad . \quad (\text{E51})$$

The vectors $\underline{\alpha}$ and \underline{r} are of the same length and since this must hold for all pairs $\underline{\alpha}$ and \underline{r} we must have that

$$M^T M = 1 \quad . \quad (\text{E52})$$

Equation (E52) also implies all eigenvalues of M are of unit magnitude. The eigenvalues and eigenvectors of M may be complex so that if $M \underline{x} = \lambda \underline{x}$, then $\underline{x}^T M^T M \underline{x} = 1 = \lambda^* \lambda \underline{x}^T \underline{x}$. For 3-dimensional space M must have at least one real eigenvalue. Since M is real, its eigenvalues must occur in complex pairs. Therefore at least one eigenvalue of M must be equal to 1. The value -1 could not be acceptable since it would imply $M \underline{u} = -\underline{u}$ which would be a reflection and already ruled out. Thus, we have that $\det M = 1$.

The matrix M is now looking very much like a rotation since the eigenvector \underline{u} is an eigenaxis. All we must do now is to determine the angle of rotation. Along with the eigenvector \underline{u} , let us define unit vectors \underline{v} and \underline{w} such that $\underline{u}, \underline{v}, \underline{w}$ is an orthonormal basis set. Also, we assume $\underline{w} = \underline{u} \times \underline{v}$. With these definitions we can express the matrix M as

$$M = M_{11} \underline{u} \underline{u}^T + M_{12} \underline{u} \underline{v}^T + M_{21} \underline{v} \underline{u}^T + \dots + M_{33} \underline{w} \underline{w}^T \quad . \quad (\text{E53})$$

From the fact that $M \underline{u} = \underline{u}$ and that $M^T M = 1$ equation (E53) reduces to

$$M = \underline{u} \underline{u}^T + p(\underline{v} \underline{v}^T + \underline{w} \underline{w}^T) + q(\underline{v} \underline{w}^T - \underline{w} \underline{v}^T) \quad ; \quad p^2 + q^2 = 1 \quad . \quad (E54)$$

We can now eliminate the vectors \underline{v} and \underline{w} from this equation by use of the proper function of \underline{u} . Thus

$$M = \underline{u} \underline{u}^T + p(1 - \underline{u} \underline{u}^T) - q \tilde{u} \quad . \quad (E55)$$

This completes the proof that the matrix M is a rotation matrix. This is now obvious from inspection of equation (E55) by comparing it to equation (E40) with $p = \cos \phi$ and $q = \sin \phi$. Thus the most general displacement of a rigid body (or transformation of a coordinate system) in which at least 1 point remains fixed is a rotation about a fixed axis i.e., the final orientation can be obtained from the original by a single rotation about the axis \underline{u} through the angle ϕ (\underline{u} and ϕ are determined from M) even though the actual motion from initial to final may have been more complex.

What all the previous discussion boils down to is that the product of a pair of rotations is itself a rotation. Thus, if M_1 and M_2 are rotations about \underline{u}_1 and \underline{u}_2 respectively, then $M_1 M_2 = M_3$ is also a rotation through some angle ϕ_3 about some axis \underline{u}_3 . In fancier terms the set of rotations forms a group under matrix multiplication.

The results of our previous discussions now suggest some new notation that may aid us in keeping up with the multiplicity of coordinate systems that must usually be dealt with in analysis of spacecraft rotational dynamics. To remain completely general, let us consider three coordinate frames A, B, C. We shall let the symbol $[BA]$ represent the rotation matrix which transforms a vector expressed in the A frame to a vector expressed in the B frame.

$$\underline{v}^{(B)} = [BA] \underline{v}^{(A)} \quad . \quad (E56)$$

For convenience we use the notation superscript (A) or (B) etc. to indicate which coordinate frames the vectors are being expressed in. If the superscripts are not specified, it means that the coordinate frame is implicit in the definition of the symbol or that it doesn't matter as long as all vectors are in the same frame. We are here more interested in the rotations $[BA]$ etc. There are three rotations between pairs: AB, BC, CA. From our previous work

$$[CA] = [CB] [BA] \quad . \quad (E57)$$

Corresponding to equation (E57) is a quaternion relation of similar form. First, since $\underline{V}^{(C)} = [CA] \underline{V}^{(A)}$, we have

$$\underline{V}^{(C)} = Q_{CA}^* \circ \underline{V}^{(A)} \circ Q_{CA} \quad . \quad (E58)$$

Here, Q_{CA} is the quaternion corresponding to $[CA]$. Thus analogous to equation (E57) we have

$$\underline{V}^{(C)} = Q_{CB}^* \circ Q_{BA}^* \circ \underline{V}^{(A)} \circ Q_{BA} \circ Q_{CB} \quad . \quad (E59)$$

Interestingly, we see that $Q_{CA} = Q_{BA} \circ Q_{CB}$ so that the factors occur in reverse order from equation (E57). However, if we use the double-bar operator we can multiply in the same order, i.e.

$$Q_{CA} = \bar{Q}_{CB} \bar{Q}_{BA} \quad . \quad (E60)$$

This result is the one which we wish to use analogous to equation (E57). Equations (E57) and (E60) have an easily remembered form and in fact behave as if multiplication cancelled the terms appearing on the inside. This makes it quite easy to construct chains of transformations to any desired system. In this notation we see that

$$[BA] = [AB]^T = [AB]^{-1} \quad ; \quad \text{also}$$

$$Q_{BA} = Q_{AB}^* = Q_{AB}^{-1} \quad . \quad (E61)$$

Finally, there are some useful tricks with the new notation we have defined. Referring to equation (E28) and adding the subscripts we have defined, we have $Q_{BA} = 0.5 Q_{BA} \circ \underline{\omega}_{BA}^{(B)}$. The vector $\underline{\omega}_{BA}^{(B)}$ is the angular velocity of B relative to A with components in B. Consider the quaternion Q_{CB} .

$$\begin{aligned}
\dot{Q}_{CB} &= \frac{1}{2} Q_{CB} \circ \underline{\omega}_{CB}^{(C)} = \frac{1}{2} Q_{CB} \circ \left(\underline{\omega}_{CA}^{(C)} - \underline{\omega}_{BA}^{(C)} \right) \\
&= \frac{1}{2} Q_{CB} \circ \underline{\omega}_{CA}^{(C)} - \frac{1}{2} Q_{CB} \circ \left(Q_{CB}^* \circ \underline{\omega}_{BA}^{(B)} \circ Q_{CB} \right) \\
&= \frac{1}{2} Q_{CB} \circ \underline{\omega}_{CA}^{(C)} - \frac{1}{2} \underline{\omega}_{BA}^{(B)} \circ Q_{CB}
\end{aligned}$$

or in matrix form

$$\dot{Q}_{CB} = \frac{1}{2} \left(\underline{\omega}_{CA}^{(C)} - \underline{\omega}_{BA}^{(B)} \right) Q_{CB} \quad . \quad (E62)$$

The utility of equation (E62) is most apparent when we use it to compute the attitude error of a spacecraft relative to a moving or moveable reference. Note that the components of $\underline{\omega}_{CA}^{(C)}$ and $\underline{\omega}_{BA}^{(B)}$ are expressed in different frames. Normally, $\underline{\omega}_{CA}^{(C)}$ would come from rate sensors which are body fixed while $\underline{\omega}_{BA}^{(B)}$ is a commanded maneuver rate which is naturally defined in the moveable reference. This equation then allows us to use both quantities directly without either being transformed.

It often becomes necessary to compute the quaternion corresponding to a given rotation matrix, i.e., find Q given $[BA]$. We have developed a computer algorithm to do this.

1) Define matrix

$$S = \left[\begin{array}{ccc|c} & & & A_{23} \\ & & & A_{31} \\ & A & & A_{12} \\ \hline -A_{32} & -A_{13} & -A_{21} & \text{tr} A \end{array} \right] ;$$

A is the given rotation.

$$2) \quad S' = S + S^T + (1 - \text{tr } A) \mathbb{I}.$$

3) $I = \max S'_{ii}$ (index of largest element along diagonal of S').

$$4) Q_j = S'_{Ij}/2 \sqrt{S'_{II}}.$$

$$5) Q'_j = Q_j \operatorname{sgn} Q_4; \operatorname{sgn} = \begin{cases} -1 & \text{for } Q_4 < 0 \\ +1 & \text{for } Q_4 \geq 0 \end{cases}.$$

Another useful and perhaps obvious technique is the expression of the quaternion resulting from a sequence of Euler rotations (rotations about coordinate axes):

$$Q_{BA} = \left(c \frac{\phi_1}{2} + \underline{u}_1 s \frac{\phi_1}{2} \right) \circ \left(c \frac{\phi_2}{2} + \underline{u}_2 s \frac{\phi_2}{2} \right) \circ \dots \\ \circ \left(c \frac{\phi_n}{2} + \underline{u}_n s \frac{\phi_n}{2} \right),$$

where $s \triangleq \sin$ and $c \triangleq \cos$. The corresponding rotation is $[BA]$ and is given by

$$[BA] = [\phi_n]_{i_n} \dots [\phi_2]_{i_2} [\phi_1]_{i_1}.$$

The vectors \underline{u} can be any of the three coordinate axes $[1,0,0]^T$, $[0,1,0]^T$ or $[0,0,1]^T$. If $\underline{u} = [1,0,0]^T$, then $i_1 = 1$, etc. We have added the convention that a rotation bracket with a subscript is an Euler rotation about the indicated axis. As an example consider the quaternion formed when $i_1 = 1$, $i_2 = 2$, $i_3 = 3$:

$$Q_{BA} = \left(c \frac{\phi_1}{2} + i s \frac{\phi_1}{2} \right) \circ \left(c \frac{\phi_2}{2} + j s \frac{\phi_2}{2} \right) \circ \left(c \frac{\phi_3}{2} + k s \frac{\phi_3}{2} \right) \\ = c \frac{\phi_1}{2} c \frac{\phi_2}{2} c \frac{\phi_3}{2} - s \frac{\phi_1}{2} s \frac{\phi_2}{2} s \frac{\phi_3}{2}$$

$$\begin{aligned}
& + i \left(s \frac{\phi_1}{2} c \frac{\phi_2}{2} c \frac{\phi_3}{2} + c \frac{\phi_1}{2} s \frac{\phi_2}{2} s \frac{\phi_3}{2} \right) \\
& + j \left(c \frac{\phi_1}{2} s \frac{\phi_2}{2} c \frac{\phi_3}{2} - s \frac{\phi_1}{2} c \frac{\phi_2}{2} s \frac{\phi_3}{2} \right) ; \\
& + k \left(c \frac{\phi_1}{2} c \frac{\phi_2}{2} s \frac{\phi_3}{2} + s \frac{\phi_1}{2} s \frac{\phi_2}{2} c \frac{\phi_3}{2} \right) ;
\end{aligned}$$

the corresponding [BA] is

$$\left[\begin{array}{c|c|c} c\phi_2 c\phi_3 & s\phi_1 s\phi_2 c\phi_3 + c\phi_1 s\phi_3 & -c\phi_1 s\phi_2 c\phi_3 + s\phi_1 s\phi_3 \\ -c\phi_2 s\phi_3 & -s\phi_1 s\phi_2 s\phi_3 + c\phi_1 c\phi_3 & c\phi_1 s\phi_2 s\phi_3 + s\phi_1 c\phi_3 \\ s\phi_2 & -s\phi_1 c\phi_2 & c\phi_1 c\phi_2 \end{array} \right] .$$

In this brief exposition, we have developed a number of useful quaternion results and notations. This by no means exhausts the possibilities. The available quaternion literature does not present the material in an easily applicable form and thus this short development is presented to fill that gap.

NOTES: The following notes apply to the previous discussion:

1) We use Q4 rather than Q0 for convenience. Since these quaternion equations will be adapted for the computer and since 0 is not usually allowed as a subscript it becomes necessary to use something else. We desire to use 1, 2, 3 for the vector components, hence Q4 is the real part;

2) The symbol $\tilde{\sim}$ is called double tilde and the symbol $\bar{\sim}$ is called double bar;

3) We shall define

$$\tilde{\tilde{Q}} = \begin{bmatrix} 0 & -Q3 & Q2 \\ Q3 & 0 & -Q1 \\ -Q2 & Q1 & 0 \end{bmatrix}$$

which is the tilde or cross product matrix for the 3-vector \underline{Q} .

APPENDIX F. ROLL COMMAND η_{xn}

To use the acquisition sun sensor (ACQ SS) for a two axes strapdown update, the sun line has to nominally pass through the center of the ACQ SS once per orbit, no matter what the tilting angle is. This can be done by rolling the vehicle about the principal x axis by the angle η_{xn} such that the vehicle z axis always has an elevation angle η_x above the orbital plane, equal to the elevation angle η_x of the sun. The transformation from the L system to the V system is ($s = \sin$, $c = \cos$)

$$[VL] \begin{bmatrix} k_{11} & k_{21} & k_{31} \\ k_{12} & k_{22} & k_{32} \\ k_{13} & k_{23} & k_{33} \end{bmatrix} \begin{bmatrix} 1 & 0 & 0 \\ 0 & c_{\eta_{xn}} & s_{\eta_{xn}} \\ 0 & s_{\eta_{xn}} & c_{\eta_{xn}} \end{bmatrix} \begin{bmatrix} c_{\eta_{zn}} & s_{\eta_{zn}} & 0 \\ s_{\eta_{zn}} & c_{\eta_{zn}} & 0 \\ 0 & 0 & 1 \end{bmatrix} \begin{bmatrix} c_{\eta_{yn}} & 0 & s_{\eta_{yn}} \\ 0 & 1 & 0 \\ s_{\eta_{yn}} & 0 & c_{\eta_{yn}} \end{bmatrix} \quad (VI)$$

from which we derive

$$VL_{32} = -s\eta_x = K_{13} s\eta_{zn} + K_{23} c\eta_{xn} c\eta_{zn} - K_{33} s\eta_{xn} c\eta_{zn} \quad ,$$

or

$$K_{33}s\eta_{xn}/R = K_{23}c\eta_{xn}/R = \eta_{xp} \quad ,$$

with

$$\eta_{xp} = (s\eta_x + K_{13}s\eta_{zn})/(Rc\eta_{zn}) \text{ and } R = \sqrt{K_{23}^2 + K_{33}^2} \quad .$$

This yields

$$\eta_{xn} = \arctan \left\{ K_{23}/K_{33} \right\} + \arctan \left\{ \eta_{xp} / \sqrt{1 - \eta_{xp}^2} \right\} \quad .$$

Inverse tangents are used since no other ARC functions are available on board. The values of the K's are given in APPENDIX G. They apply for the EOVV A orientation. For the EOVV B orientation we have

$$[K]_B = \begin{bmatrix} -1 & 0 & 0 \\ 0 & -1 & 0 \\ 0 & 0 & 1 \end{bmatrix} [K]_A$$

i.e., K_{13} and K_{23} change sign.

APPENDIX G. DATA

Vehicle moments of inertia matrix (kgm^2)

$$I_V = \begin{bmatrix} 894828 & -63414 & -529360 \\ -63414 & 3763111 & -27295 \\ -529360 & -27295 & 3598005 \end{bmatrix} .$$

Principal moments-of-inertia matrix (kgm^2)

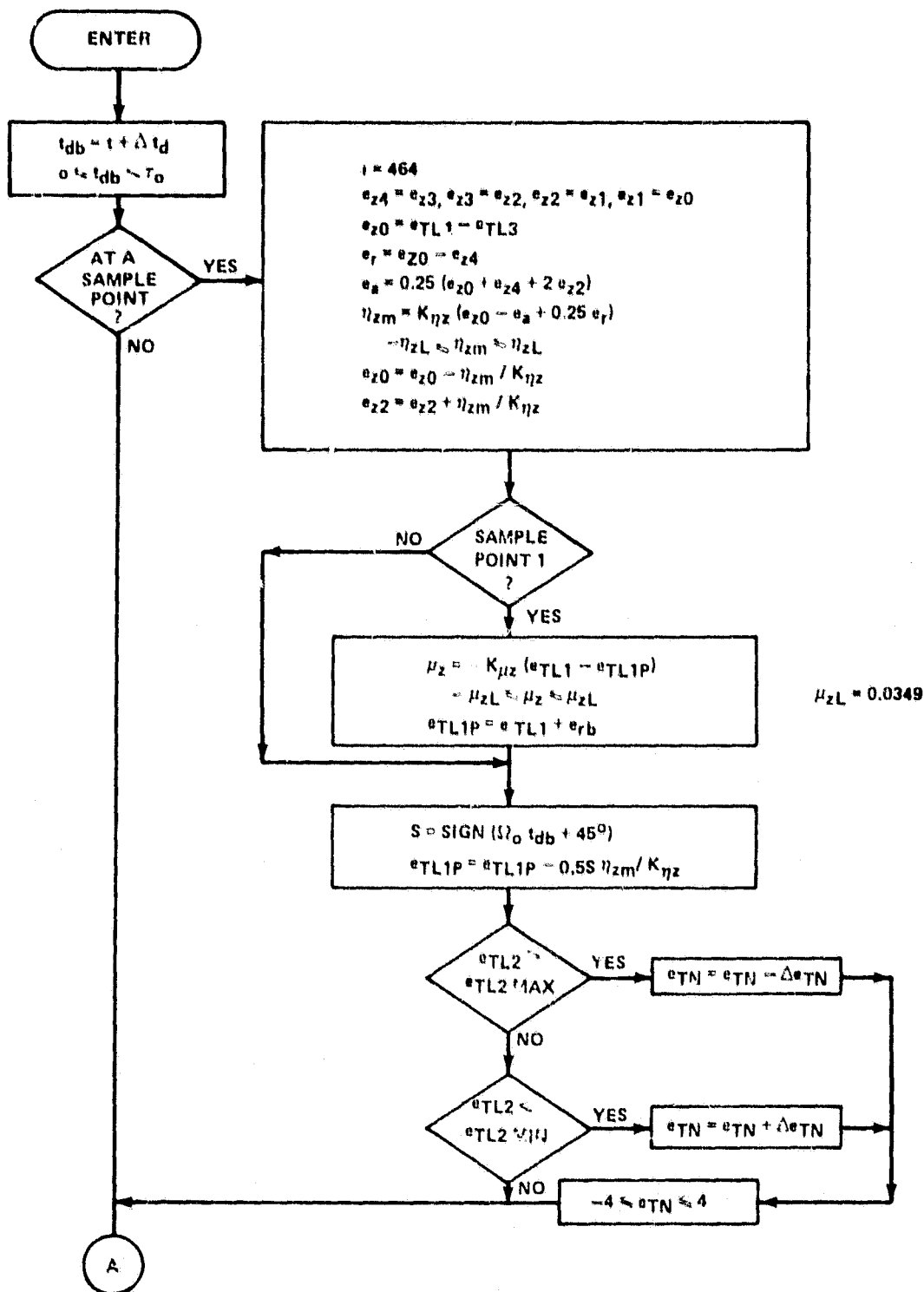
$$I_P = \begin{bmatrix} 793332 & 0 & 0 \\ 0 & 3767879 & 0 \\ 0 & 0 & 3694732 \end{bmatrix}$$

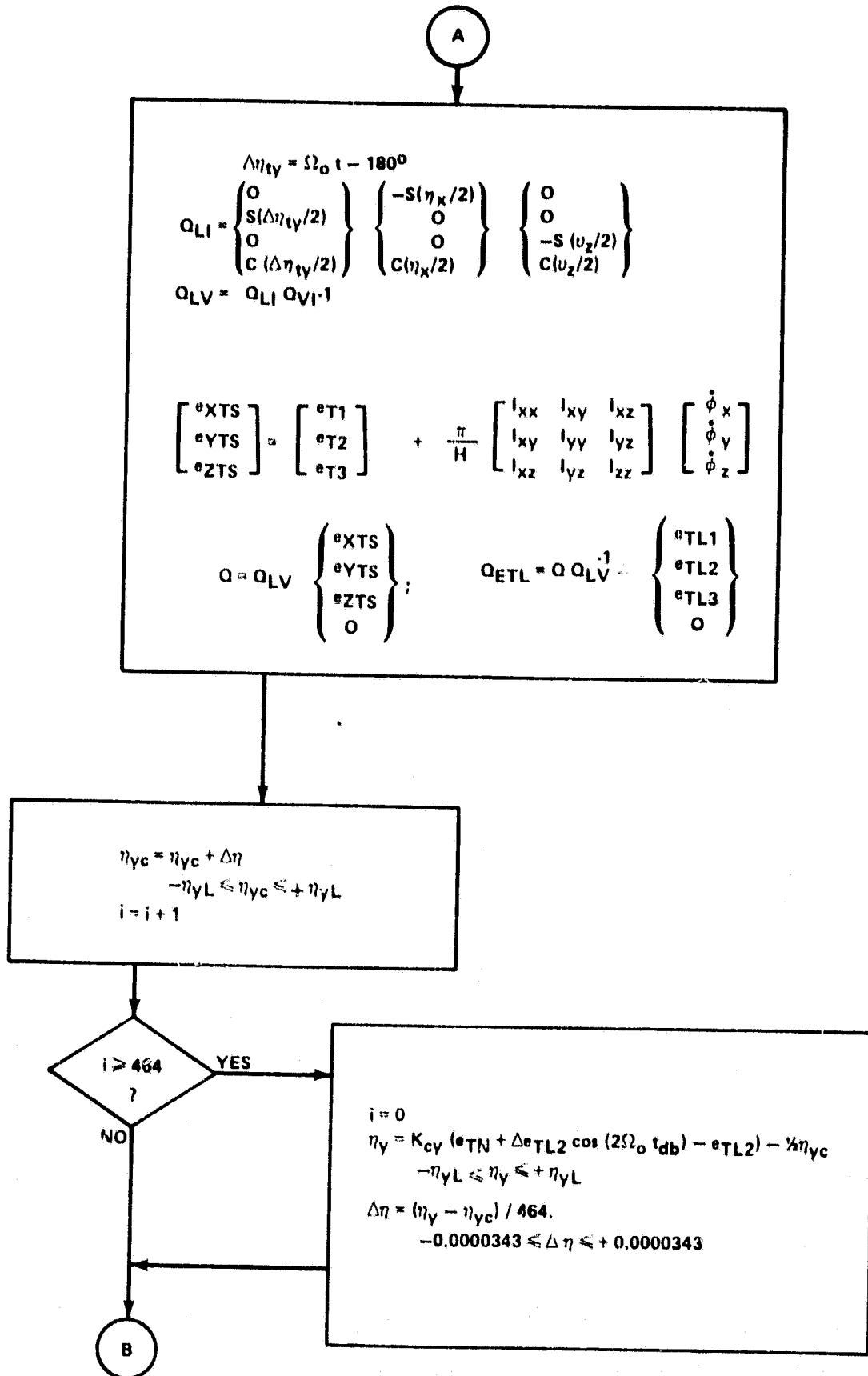
Transformation from vehicle to principal coordinate system

$$[K] = [PV] = \begin{bmatrix} 0.982357 & 0.022682 & 0.185632 \\ 0.017288 & 0.977351 & -0.210913 \\ -0.186213 & 0.210401 & 0.959716 \end{bmatrix} .$$

APPENDIX H. FLOWCHARTS

MANEUVER REQUIREMENTS





B

$$\eta_{yn} = \eta_{yc} - \eta_{ym} \sin(2\Omega_o t_{db})$$

$$\eta_{zn} = -\eta_{zm} \sin(2\Omega_o t_{db})$$

$$E_{K13} = \begin{cases} +0.185633 & \text{IF } EOVB \text{ FLAG} = 0 \\ -0.185633 & \text{IF } EOVB \text{ FLAG} \neq 0 \end{cases}$$

$$\eta_{xp} = (\sin \eta_x + E_{K13} \sin \eta_{zn}) / (0.982619 \cos \eta_{zn})$$

$$\eta_{xn} = \text{ARCTAN}(\eta_{xp} / (1 - \eta_{xp}^2)^{1/2})$$

$$\eta_{xn} = \begin{cases} \eta_{xn} - 12.396^\circ & \text{IF } EOVB \text{ FLAG} = 0 \\ \eta_{xn} + 12.396^\circ & \text{IF } EOVB \text{ FLAG} \neq 0 \end{cases}$$

$$Q_N = \begin{Bmatrix} \sin \eta_{xn}/2 \\ 0 \\ 0 \\ \cos \eta_{xn}/2 \end{Bmatrix} \begin{Bmatrix} 0 \\ 0 \\ \sin \eta_{zn}/2 \\ \cos \eta_{zn}/2 \end{Bmatrix} \begin{Bmatrix} 0 \\ \sin \eta_{yn}/2 \\ 0 \\ \cos \eta_{yn}/2 \end{Bmatrix}$$

$$Q_{BL} = Q_M Q_N$$

$$r_1 = 2(q_{BL1} q_{BL2} + q_{BL3} q_{BL4})$$

$$r_2 = (q_{BL2}^2 - q_{BL1}^2 - q_{BL3}^2 + q_{BL4}^2)$$

$$r_3 = 2(q_{BL3} q_{BL2} - q_{BL1} q_{BL4})$$

$$\Omega_b = (1 - 2\eta_{ym} \cos(2\Omega_o t_{db}))$$

$$\dot{\theta}_x = r_1 \Omega_o \Omega_b$$

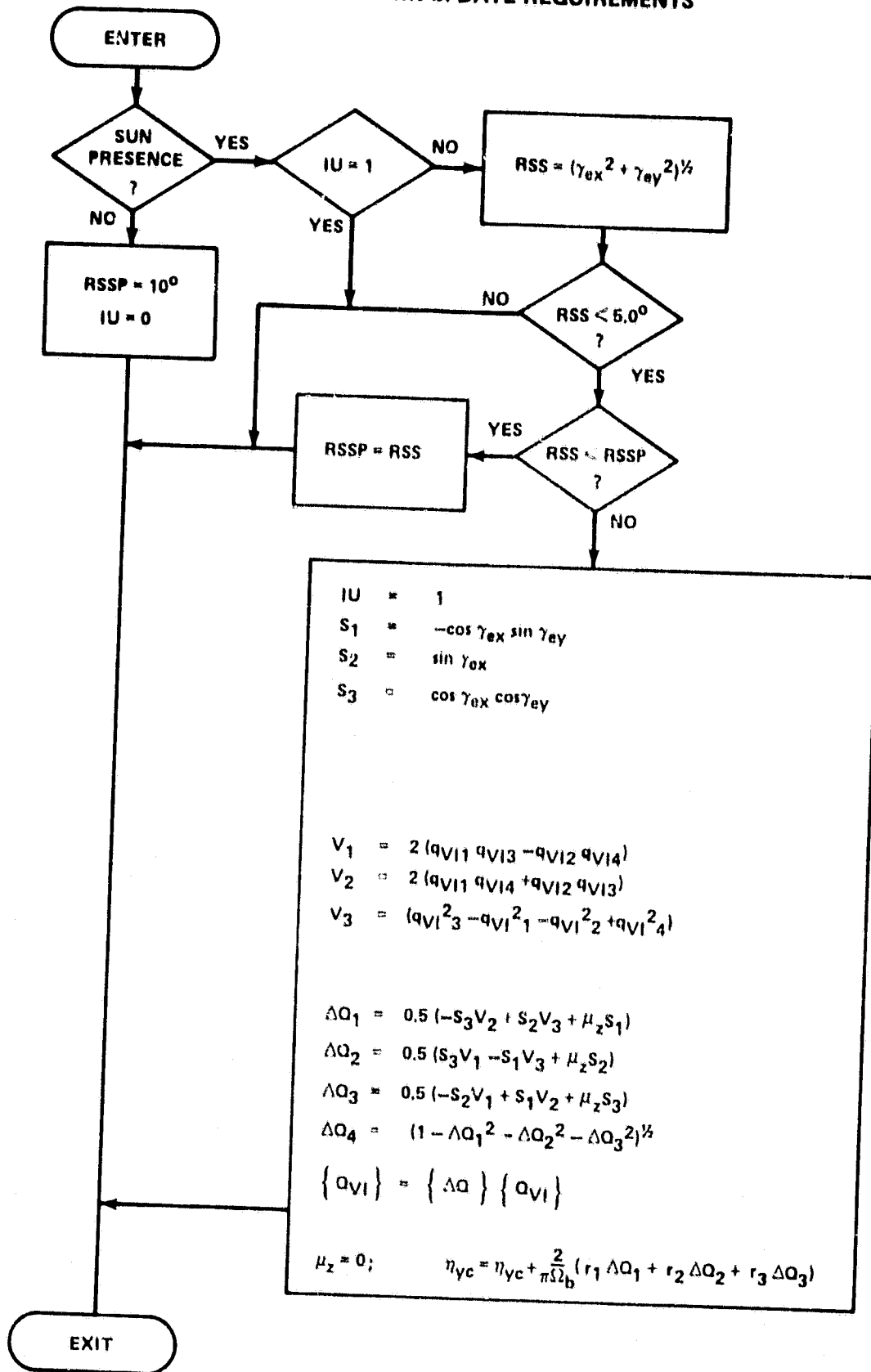
$$\dot{\theta}_y = r_2 \Omega_o \Omega_b$$

$$\dot{\theta}_z = r_3 \Omega_o \Omega_b$$

$$Q_{AI} = Q_{BL} Q_{LI}$$

EXIT

STRAPDOWN UPDATE REQUIREMENTS



REFERENCES

1. Glaese, J.R. and Kennel, H.F.: Torque Equilibrium Attitude Control for Skylab Reentry. NASA TM-78252, November 1979.
2. Chubb, W.B.: Skylab Reactivation Mission Report. NASA TM-78267, March 1980.
3. Chubb, W.B. et al: Flight Performance of Skylab Attitude and Pointing Control System. NASA TN D-8003, June 1975.
4. Kennel, H.F.: A Control Law for Double-Gimbaled Control Moment Gyros Used for Space Vehicle Attitude Control. NASA TM X-64536, August 7, 1970.
5. ATMDC Program Definition Document. IBM NO 70-207-0002, May 10, 1973.
6. Kennel, H.F.: Angular Momentum Desaturation for Skylab Using Gravity Gradient Torques. NASA TM X-64628, December 7, 1971.